

AD-A052 020

BROWN UNIV PROVIDENCE R I DEPT OF CHEMISTRY
FAR INFRARED AND RAMAN SPECTRA AND ION MOTION IN SODIUM-BETA-AL--ETC(U)
DEC 77 W M BUTLER, W M RISEN

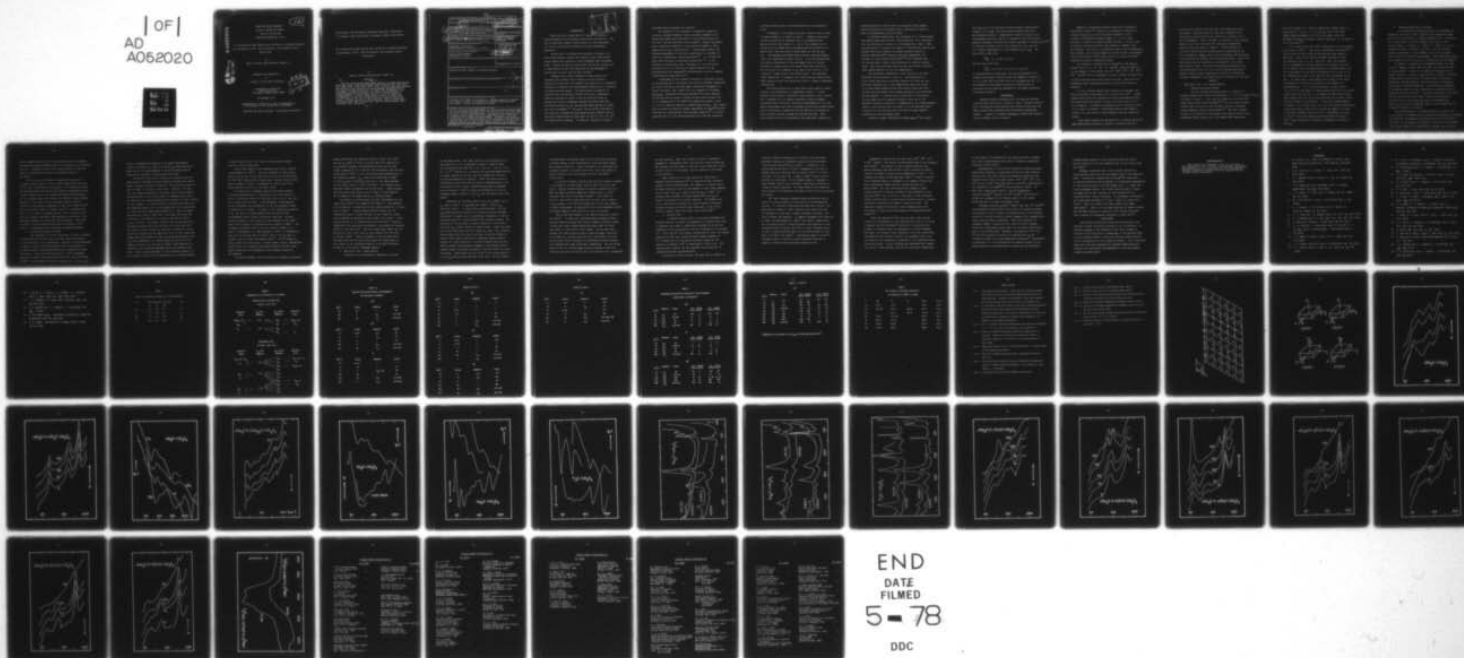
N00014-75-C-0883

NL

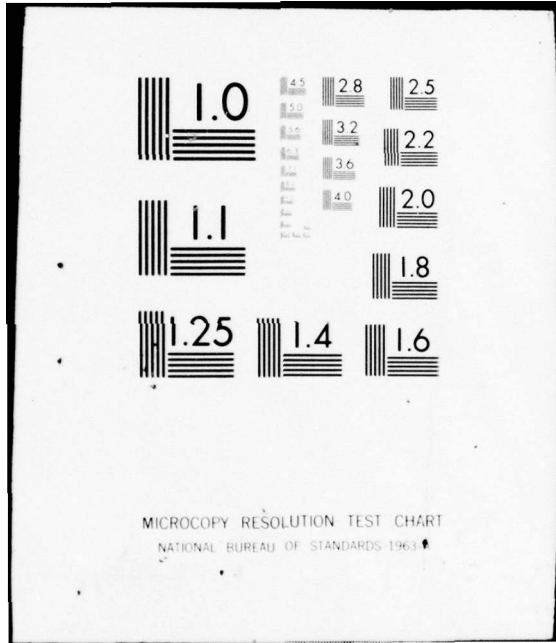
UNCLASSIFIED

TR-77-04

| OF |
AD
A052020



END
DATE
FILMED
5 - 78
DDC



MICROCOPY RESOLUTION TEST CHART
NATIONAL BUREAU OF STANDARDS-1963-A

12_{sc}

AD A 052020

OFFICE OF NAVAL RESEARCH

Contract N00014-75-C-0883

Task No. NR 051-539

TECHNICAL REPORT NO. 77-04

Far Infrared and Raman Spectra and Ion Motion in Sodium- β -Alumina,
its Potassium, Silver, Thallium Analogs, and Divalent Cation
Derivatives

by

Wayne M. Butler and William M. Risen, Jr.

AD NO. []
DDC FILE COPY

Prepared for Publication

in

Journal of Solid State Chemistry

Department of Chemistry
Brown University
Providence, Rhode Island 02912

DDC
APR 3 1978
F

26 December 1977

Reproduction in whole or in part is permitted for
any purpose of the United States Government

Approved for Public Release: Distribution Unlimited

Contribution from the Metcalf Research Laboratory, Department
of Chemistry, Brown University, Providence, Rhode Island 02912

Far Infrared and Raman Spectra and Ion Motion in Sodium- β -Alumina,
its Potassium, Silver, Thallium Analogs, and Divalent Cation
Derivatives

by

Wayne M. Butler and William M. Risen, Jr.

Abstract

The far infrared and laser Raman spectra of cation-substituted materials based on sodium β -alumina containing K^+ , Rb^+ , Cs^+ , Ag^+ , Tl^+ , Ca^{+2} , Sr^{+2} , Pb^{+2} , Mn^{+2} , Fe^{+2} , Co^{+2} , and Ni^{+2} have been obtained. The materials were prepared by ion-exchanging sodium- β -alumina with pure or mixed molten salts of these ions according to the Yao-Kummer and Harata methods. The spectra were obtained at various degrees of cation substitution so that the growth at disappearance of spectral bands could be used to assign them to vibrations of the ions to the different types of sites they occupy. Through the use of this technique, cation vibrations at mid-oxygen (mO), Beever-Ross (BR), and anti-Beever-Ross (aBR) sites have been identified.

SECURITY CLASSIFICATION OF THIS PAGE (When Data Entered)

9 Technical rept.

REPORT DOCUMENTATION PAGE

READ INSTRUCTIONS BEFORE COMPLETING FORM

1. REPORT NUMBER	2. GOVT ACCESSION NO.	3. RECIPIENT'S CATALOG NUMBER
beta		14 TR-77-04

4. TITLE (and Subtitle)	5. TYPE OF REPORT & PERIOD COVERED
6 Far Infrared and Raman Spectra and Ion Motion in Sodium- β -Alumina, its Potassium, Silver, Thallium Analogs, and Divalent Cation Derivatives.	

7. AUTHOR(s)	8. CONTRACT OR GRANT NUMBER(s)
10 Wayne M./Butler and William M./Risen, Jr.	15 N 000 14-75-C-0883 NR 051-539

9. PERFORMING ORGANIZATION NAME AND ADDRESS	10. PROGRAM ELEMENT, PROJECT, TASK AREA & WORK UNIT NUMBERS
Department of Chemistry Brown University, Providence, R. I. 02912	12 57p.

11. CONTROLLING OFFICE NAME AND ADDRESS	12. REPORT DATE
Office of Naval Research Department of the Navy	11 26 Dec 1977

14. MONITORING AGENCY NAME & ADDRESS (if different from Controlling Office)	13. NUMBER OF PAGES
	59
	15. SECURITY CLASS. (of this report)
	15a. DECLASSIFICATION DOWNGRADING SCHEDULE

16. DISTRIBUTION STATEMENT (of this Report)

Approved for Public Release: Distribution Unlimited

17. DISTRIBUTION STATEMENT (of the abstract entered in Block 20, if different from Report)

18. SUPPLEMENTARY NOTES

19. KEY WORDS (Continue on reverse side if necessary and identify by block number)

β -alumina, beta-alumina, ionic conductors, superionic conductors, potassium ion, sodium ion, silver ion, thallium ion, transition metal-substituted beta-alumina, divalent ion-substituted β -alumina.

20. ABSTRACT (Continue on reverse side if necessary and identify by block number)

The far infrared and laser Raman spectra of cation-substituted materials based on sodium β -alumina containing K^+ , Rb^+ , Cs^+ , Ag^+ , Tl^+ , Ca^{+2} , Sr^{+2} , Pb^{+2} , Mn^{+2} , Fe^{+2} , Co^{+2} , and Ni^{+2} have been obtained. The materials were prepared by ion-exchanging sodium- β -alumina with pure or mixed molten salts of these ions according to the Yao-Kummer and Harata methods. The spectra were obtained at various degrees of cation substitution so that the growth at disappearance of spectral bands could be used to assign them to vibrations of the ions to the different types of sites they occupy. Through the use of this technique,

405 436- You

INTRODUCTION

ACCESS: for	White Section <input checked="" type="checkbox"/>	Buff Section <input type="checkbox"/>
NTIS		
DDC		
UNANNOUNCED		
JUL 1 1964		
BY	DISTRIBUTION/AVAILABILITY CODES	
Dis...	SP-CIAL	
A		

There has been a great deal of interest in sodium β -alumina because of its unusually high sodium ion mobility. This and its excellent thermal stability have in turn encouraged its use as a solid state electrolyte in high temperature batteries.¹

Sodium ions in β -alumina are contained in planes of Na and O which separate spinel-like blocks of four close packed oxygen layers with aluminum in both octahedral and tetrahedral holes. Sodium ion motion occurs within the Na and O planes and is sufficiently facile that sodium may be ion-exchanged in molten salts of mono- and divalent cations.²

Although only silver- β -alumina of these analogs has reported ionic conductivity as high as sodium- β -alumina, substitution with other ions permits the observation of systematic variations in physical and spectroscopic properties as a function of cation size and charge. The spectroscopic properties of interest here are the mobile cation vibrational frequencies which are expected to occur in the far infrared region by analogy with similar condensed systems³ and which have been previously observed in the infrared and Raman spectra of sodium and silver- β -alumina.^{4,5} We report the ion motion frequencies and other far infrared and laser Raman spectra features and the structural implications of these data for the K^+ , Ag^+ , Tl^+ , Rb^+ , Cs^+ -substituted β -aluminas. In addition, spectra of divalent

ion-substituted β -aluminas are reported.

All theories of ion transport in superionic conductors invoke an "attempt frequency" which presumably depends on all vibrational modes which contribute to the diffusive motion of the ions. The Rice and Roth free-ion model⁶ relates the ground state vibrational frequency to the activation energy of ionic conduction in ionic oxide glasses.⁷ Other models explain the frequency dependence of the ionic conductivity in β -alumina in terms of a conventional random walk model^{8,9} or a random walk model with inclusion of many-body interactions.¹⁰ In fact, cooperative interactions play a dominant role in lowering the Coulombic barrier to diffusion in domain models¹¹ and the interstitialcy pair mechanism¹², which predicts that the resonant frequencies will not scale $M^{-1/2}$.

A knowledge of the β -alumina structure is obviously crucial to any explanation of ion motion, yet the very disorder responsible for facile ion motion has precluded a definitive assignment of cation locations. The "ideal" unit cell formula of β -alumina, $\text{Na}_2\text{Al}_{22}\text{O}_{34}$, determined by Beevers and Ross,¹³ is never observed in practice and is actually outside the equilibrium phase field at all temperatures.¹⁴ At 1700°C the composition range is from $x = 1.2-1.5$ using the empirical formula $x\text{Na}_2\text{O} \cdot 11\text{Al}_2\text{O}_3$. This implies that an excess of sodium is charge compensated by oxygen¹⁵ although there may be a contribution from aluminum vacancies.¹⁶ It is also apparent that not only the stoichiometry but also the conditions

of crystal growth affect the microstructure of the conduction plane.

A schematic of the conduction plane, which is also a plane of mirror symmetry, is shown in Figure 1. Oxygen in the plane is held in position by aluminum ions in tetrahedral holes above and below each oxygen ion. One of the possible sets of cation sites is symbolized by triangles and are referred to as Beevers-Ross (BR) positions of which there are two per unit cell. Surrounding each Beevers-Ross site are three mid-oxygen sites (mO) symbolized by small circles. As in the BR positions, the cation coordination at the mid-oxygen sites is trigonal prismatic to oxygen ions in the spinel block above and below, but the actual site symmetry is C_{2v} due to the location of two "separator" oxygen atoms in the mirror plane. The remaining sites, symbolized by hexagons, are called the anti-Beevers-Ross (aBR) positions where the cations are held in trigonal bipyramidal coordination.

The cation population at these three sites found by single crystal x-ray diffraction is summarized in Table I. Cation density is not sharply localized at these specific sites, however, but is smeared out in a highly anisotropic fashion probably reflecting both vibrational and static displacements of the ions. These displacements are most pronounced in thallium- β -alumina where most of the density associated with the aBR site is centered at points halfway between the aBR site and mO positions. Both thallium and silver are stabilized at the aBR sites, probably by

forming partially covalent bonds to the spinel block oxygens above and below, but the larger steric repulsions of thallium make its displacements more noticeable.

At elevated temperatures, the occupancy of all sites becomes more nearly equal and the ionic "delocalization" is so pronounced that the structure is similar to a two-dimensional liquid. Here, "delocalization" is used in the sense of a distribution density map. Neutron diffraction studies on sodium- β -alumina crystals at various temperatures¹⁵ illustrate this most graphically, but analysis of x-ray diffuse scattering^{21,22} also indicates that the cations adopt a quasi-liquid structure at elevated temperatures. The x-ray work also indicates that the cations form short range ordered domains at very low temperatures.

The vibrational symmetries of ions located at the three different sites are given in Table II. The possibility of factor group splitting is uncertain because all sites are only partially occupied, but at low temperatures where the all-BR or all-mid-oxygen domains become sufficiently large and interactions along the domain walls become negligible, such splitting may be observed. It should also be noted that if the cations on BR or aBR sites are displaced slightly along one of the threefold diffusive pathways as is suggested in the crystallographic studies, the displaced ions will form, on a time averaged basis, a manifold of six sites per unit cell with the same symmetry properties as the mid-oxygen sites.

Potential energy calculations by Wang et al.¹² have shown

that when two of the threefold mO sites around a Beavers-Ross vacancy are occupied, the four nearest cations on BR sites are displaced slightly. Experimental evidence for such static displacements has been obtained in studies of the ^{23}Na nuclear magnetic resonance linewidth and electric quadrupole interaction.^{23,24} In the most favorable case of non-interacting ions, each ion will vibrate independently in site symmetry C_{2v} or D_{3h} . For ions on BR or aBR sites

$$\Gamma_{\text{vib}}^{D_{3h}} = E' (ir, R) + A_2'' (ir)$$

and for ions on mO sites

$$\Gamma_{\text{vib}}^{C_{2v}} = A_1 (ir, R) + B_1 (ir, R) + B_2 (ir, R)$$

If interactions are significant, the non-stoichiometry of β -alumina would almost certainly lower the symmetry of each ion to C_s so that each site would have the representation $2A' + A''$. We attempted to distinguish between the possibilities by analyzing the polarization dependence of the Raman scattering from single crystals.

EXPERIMENTAL

Powdered sodium β -alumina with 7.4% Na_2O was obtained from the Alcoa pilot plant in East St. Louis. Ground β -alumina with 6.2% Na_2O and large crystals for infrared reflectance and Raman studies were purchased from the Harbison Carborundum Company. A sample of rubidium exchanged β -alumina was obtained from the General Electric Company.

Samples of intermediate sodium content were prepared by the method of Harata.²⁵ Mixtures of β -alumina of composition $1.2\text{Na}_2\text{O} \cdot 11\text{Al}_2\text{O}_3$ plus sufficient sodium carbonate to give ultimate stoichiometries $x\text{Na}_2\text{O} \cdot 11\text{Al}_2\text{O}_3$ ($x = 1.2-1.8$) were preheated to 1000°C in sealed platinum crucibles. Pellets 15mm in diameter and 3mm thick were then pressed at 30000psi from the mixtures. The pellets, covered with some of the corresponding loose powder, were tightly wrapped in several layers of molybdenum foil and sintered at 1700°C under argon in an Astro ultra-high temperature graphite resistance furnace.

The sodium in β -alumina was so exchanged to the maximum extent with Li^+ , K^+ , Cs^+ , Ag^+ , Tl^+ , and NH_4^+ using the methods of Yao and Kummer.² The divalent ions Ca^{2+} , Mn^{2+} , Fe^{2+} , Co^{2+} , Ni^{2+} , Sr^{2+} , and Pb^{2+} were so exchanged to various extents in mixed melts of sodium chloride and divalent metal chloride. The salts were dehydrated under vacuum and melted in sealed quartz tubes at $950 \pm 20^\circ\text{C}$.

All far infrared spectra were recorded on a Digilab, Inc. FTS-14 infrared interferometer at a resolution of 4cm^{-1} . Powder samples were mixed with powdered low density polyethylene which was then melted and pressed to form a thin wafer four or five cm in diameter. Low density polyethylene has no absorption bands in the region of interest. Reflectance spectra were taken of crystals, at least 5mm on a side, parallel with the conducting planes.

Laser Raman spectra were measured with a Jarrell-Ash 25-300 Raman spectrometer operated at ca 3cm^{-1} resolution and 1cm^{-1}

accuracy using various exciting lines from krypton and argon ion lasers. Scattered light was optically scrambled after polarization analysis and before passing the entrance slit of the monochromator. Since β -alumina is isotropic in the xy-plane, there are only four different 90° scattering arrangements possible which are shown in Figure 2. The excitation and collection directions and polarizations are described by the usual convention, $\underline{i}(\underline{k}\underline{\ell})\underline{j}$, where \underline{i} and \underline{j} represent the directions of polarization of incident and scattered radiation, respectively, and \underline{k} and $\underline{\ell}$ are the directions of polarization of incident and collected light. The measured scattering intensities are only qualitative since all the crystals used had macroscopic defects, which caused a significant variation in scattering intensity depending on the exact point of incidence of the laser.

RESULTS

A. Monovalent Ions - Far Infrared Spectra

1. Sodium-containing Aluminas

The far infrared absorption spectra of samples of sodium- β -alumina with nominal stoichiometry $x = 1.2-1.8$ in $x\text{Na}_2\text{O} \cdot 11\text{Al}_2\text{O}_3$ are shown in Figure 3. This range of composition is within the single phase region found by Harata,^{25,26} but the highest sodium content sample would be in the two phase region of β -alumina-sodium aluminate found by other workers.²⁷ The most striking feature of the spectra is the growth of the band at 113cm^{-1} with increasing sodium content until the sodium oxide content per

unit cell reaches 1.6. Since no significant change occurs on going from $x = 1.6$ to $x = 1.8$ in the top trace, this high sodium sample presumably lies in the two phase region and although the amount of NaAlO_2 formed is uncertain, it is expected to be very small.²⁸

It is notable that the 113cm^{-1} band grows in at the expense of the band at 87cm^{-1} . This can be explained by recalling^{11,12} that cations are most stable at BR sites and least stable at aBR sites. Since steric effects prohibit occupancy of any two adjacent sites (i.e. mO - BR or mO - aBR), the simplest way to accommodate an excess sodium ion in a planar unit cell is to displace the ion already present on the Beevers-Ross site to a mid-oxygen site and place the additional Na on one of the two remaining mO sites of the threefold set surrounding the BR site. In other words, each sodium ion in excess of the ideal stoichiometry is likely to be present as one member of a mid-oxygen pair. If x is the total amount of Na_2O present, $4(x-1)$ will be the amount of sodium present per unit cell on mid-oxygen sites and $4-2x$ will be the amount on Beevers-Ross sites. This accounts well for the cation distributions of Table I where covalent bonding is unimportant. In the Na- β -alumina samples of Figure 1, as x varies from 1.2 to 1.6, the sodium concentration on mO sites varies from 0.8 to 2.4 while the amount of sodium on BR sites decreases from 1.6 to 0.8. Accordingly, the band at 113cm^{-1} arises from sodium on mO sites while the band at 87cm^{-1} which decreases in intensity corresponds to sodium on BR sites.

2. Potassium-substituted β -alumina

In β -alumina with sodium progressively exchanged for potassium, the band at 87cm^{-1} persists while additional bands grow in at 72 and 109cm^{-1} at higher exchange levels. Potassium ion is more stable in solid β -alumina than sodium in the ternary system: β -alumina (s) - KNO_3 (l) - NaNO_3 (l); so the spectrum in Figure 4 labeled 5 mole %K in the nitrate melt actually corresponds to 25% exchange in the solid β -alumina, while a 50% melt indicates 80% exchange. Phase equilibria curves for a number of melts are given in the paper by Yao and Kummer.²

In samples of completely K^+ -exchanged alumina, the band at 87cm^{-1} remains stronger than the other two ion motion bands at 72 and 109cm^{-1} . Since the β -alumina stoichiometry of all samples requires 1.2 moles of M_2O per mole of sample, the amount of potassium on BR sites will be greater than on mO sites in completely exchanged samples, and this should be reflected in the relative infrared intensities. The vibrational frequency of potassium on BR sites must therefore be coincident with the sodium BR vibration at 87cm^{-1} . The bands which grow in on either side of this at 72cm^{-1} and 109cm^{-1} arise from potassium on mO sites and in factor group D_{6h} would be designated A_{2u} and/or E_{1u} but may be considered simply as the in-phase and out-of-phase vibrations of mO pairs.

The disappearance of the sodium mO band at 113cm^{-1} even at low levels of exchange can be explained by assuming the potassium ions initially exchanged are distributed over both the BR and mO sites. At low degrees of exchange, potassium on a mid-oxygen site is most likely to be paired with a sodium, and the inter-

action between the two ions of this mixed mO pair will broaden the absorption bands characteristic of all-sodium or all-potassium mO pairs. Potassium on BR sites is sufficiently far from the nearest occupied sites so that the broadening effect is negligible.

That the ionic vibrations of sodium and potassium in β -alumina should appear to be so little influenced by the mass of the ions is explained by the nature of the conducting planes. The spacing between the spinel-like blocks is determined by the "spacer" oxygen ions in the conducting planes in Na- β -alumina, but for cations larger than sodium, the cationic radius becomes dominant.² The effect of this increased lattice strain is observed in the pressure dependence of the ionic conductivity²⁹ and in the spectra shown in Figure 5 which is a superposition of Na, K, Rb, and Cs- β -alumina spectra. The ion motion bands display an almost negligible mass dependence indicating a size dependent increase in vibrational force constants. (The band at 167cm^{-1} in Na- β -alumina which varies strikingly in this series is a deformation mode involving aluminum and oxygen.)

3. Silver-substituted- β -alumina

The assignment of cation vibrations in silver β -alumina is complicated by the fact that all three sites are occupied as was discussed in the Introduction. Spectra of silver exchanged β -alumina in melts containing 2-20 mole %Ag corresponding to β -alumina samples containing 60-90% silver exchanged are shown in Figure 6. Since over half the silver in fully exchanged samples is found at the Beevers-Ross positions, the strong band at 38cm^{-1} is attributed to silver on these sites. At the lowest

degree of exchange this appears as two bands representing either the in-plane E_{1u} and out-of-plane A_{2u} bands expected or bands due to the lower symmetry of partial exchange such as preferential occupancy of displaced BR positions.

One third of the silver ultimately is found at the anti-Beevers-Ross sites where covalent bonding contributions should impart a higher vibrational frequency. We therefore assign the band at 74cm^{-1} to silver on these sites. However, this band does not change appreciably in intensity with further exchange, indicating that at the lowest degree of exchange shown ($\sim 60\%$), the aBR sites are already saturated with respect to their ultimate silver occupancy. If silver initially occupies only aBR sites, the remaining sodium ion of a mid-oxygen site pair is permitted to occupy the more stable Beevers-Ross site. Since the known population of silver on aBR sites is not much less than that on BR sites, the stability of the two sites must be nearly equal for silver. For sodium, however, the Coulomb potential difference between the BR and mO sites is greater than 1eV .¹⁴ The overall crystal energy can therefore be lowered if silver initially occupies only the aBR sites until all the sodium mid-oxygen pairs are reduced to singly occupied Beevers-Ross sites. Using this hypothesis, no sodium remains on mO sites in the samples of Figure 6 so the band at 123cm^{-1} which declines in intensity with increasing exchange arises from sodium at BR sites. The increased frequency of this vibration relative to pure sodium β -alumina may be explained by the covalent bonding

induced contraction of the c-axis in Ag- β -alumina brought about by silver at aBR sites.

Even in the samples fully exchanged with silver, however, a band remains at 112cm^{-1} . From its intensity and position we assign this to the out-of-plane mode of silver on the aBR sites and the 74cm^{-1} band as the in-plane mode. Another feature which grows in weakly at 84cm^{-1} is assigned to silver on mO sites which account for 10-15% of the total silver.

To confirm this assignment and to distinguish between vibrations perpendicular to and parallel with the conduction planes, reflectance spectra of the (001) face of Na, K, Ag, and Tl- β -alumina were recorded. A Kronig-Kramers transformation was not performed since dispersion in the low frequency region is expected to be slight. In Figure 7, the transmission spectra of Na, Ag, and Tl- β -alumina powders are traced above the corresponding single crystal reflectance spectrum. The most striking feature of these spectra is the weakness of the 87cm^{-1} band of Na- β -alumina in reflectance which appears at 96cm^{-1} . The strongest reflectance peak in the low frequency region is at 47cm^{-1} corresponding to a weak shoulder at 55cm^{-1} in transmission. From this we conclude that the 87cm^{-1} band is the A_{2u} mode of sodium on BR sites while the band at 55cm^{-1} is the in-plane E_{1u} mode of sodium on those sites. A recent single crystal transmittance study³⁰ with a far infrared laser beam colinear with the c-axis found a band near this frequency as the strongest feature in the spectrum.

In silver β -alumina, the two strong low frequency reflectance

peaks confirm that the absorption bands at 38cm^{-1} and 74cm^{-1} are the E_{1u} modes of silver on BR and aBR sites respectively. In thallium β -alumina, the Beevers-Ross sites are the most highly occupied and it is obvious from the spectra that the very strong band at 97cm^{-1} is the vibrational mode perpendicular to the conduction planes, A_{2u} , while the strong band at 48cm^{-1} is the E_{1u} mode of thallium on BR sites. The weak shoulders on this latter band, at 31cm^{-1} and 60cm^{-1} , are probably due to thallium slightly displaced from the BR sites. Bands arising from thallium on aBR sites are not evident in these spectra but do appear in the Raman spectra as discussed below.

The observed infrared bands and their assignments for the region below 250cm^{-1} are summarized in Table II. The spectrum of Li- β -alumina is featureless in this region except for a lattice mode at 219cm^{-1} . Lithium samples hydrate readily and the interstitial water is bound strongly in the conduction planes thus broadening an inherently broad signal even further. Transmission spectra of all samples were also recorded at liquid N_2 temperature with negligible sharpening of the bands and frequency shifts of less than 3cm^{-1} . The only significant change was the splitting of the 112cm^{-1} band in Ag- β -alumina into two bands at 108 and 115cm^{-1} . There is probably a lattice mode nearly coincident with the ion motion band since two bands appear in this region in the reflectance spectra of Na and K- β -alumina as well as in the silver exchanged samples.

B. Monovalent Ions - Raman Spectra

Although ion motion bands are expected to be weak

in the Raman effect, the large variation in polarizability in the series Na, K, Ag, Tl provides a means to identify them. The polarizabilities in Å^3 are: Na = 0.41, K = 1.33, Ag = 2.4, Tl = 5.2.³¹ Figures 3-10 illustrate the polarized Raman spectra of single crystals of Na, Ag, and Tl- β -alumina for the four scattering geometries of Figure 2. Since the crystal must be reoriented in going from the top pair of configurations to the bottom pair in each figure, intensities may only be compared within each pair. Table IV lists the intensities in the low frequency region relative to the A_{1g} Al-O deformation mode near 260cm^{-1} .

Recurring low frequency modes in all four samples are an A_{1g} band at 84cm^{-1} , an E_{2g} band near 100cm^{-1} , and an E_{1g} band near 115cm^{-1} . Of these three recurring modes, only the A_{1g} shows negligible variation in relative intensity through the series of samples and is accordingly assigned as a lattice mode which does not involve atoms in the conduction plane. The intensity of the E_{1g} mode is greatly enhanced in silver-beta while the E_{2g} is most intense in thallium-beta. These two bands are clearly associated with the conduction plane, and, although phonon modes (such as spinel block shear along the conduction planes) might remain unshifted in frequency despite notable changes in c-axis dimension if covalent bonding involving the mobile cations counterbalances changes in the cohesive forces between blocks, we assign the bands at 100 and 115cm^{-1} as cation vibrations. These modes (100 and 115cm^{-1}) are strong relative to the E_{2g} mode arising from ions on BR sites, but this results

the more highly constrained ions at mO or aBR sites effecting a greater change in the polarizability along the metal-oxygen axis during a vibration. These two bands in Na and K-beta are assigned as modes of cations on mO sites since they appear at higher frequency than the BR modes at 60cm^{-1} and 69cm^{-1} , respectively.

In silver- β -alumina, the mO sites are only slightly occupied, so the bands at 103 and 111cm^{-1} must be due to silver at aBR sites. Partial covalent bonding of silver at these sites will make the Raman scattered bands more intense and at a higher frequency than the BR site mode at 24cm^{-1} . From Table II, however, ions on BR or aBR sites will not give rise to modes of E_{1g} symmetry, but this rule breaks down if the ions undergo a static displacement as suggested by the crystallographic results and assume symmetry rules similar to ions on mO sites.

Two strong bands appear in the thallium spectra at 165cm^{-1} and 197cm^{-1} . If these were aluminum-oxygen deformation modes (greatly enhanced because they involve oxygen covalently bonded to thallium) similar modes should have been found in silver-beta which is featureless in this region. We are thus led to surmise that these bands are due to thallium-oxygen vibrations at the aBR site, because only this site can produce the close metal-oxygen contact necessary for pronounced covalent bonding and commensurately high vibrational frequencies. The two strong bands in the far infrared spectrum were assigned to thallium vibrations on only one type of site, but one site can't accommodate

all the thallium. Thus, the ir band at 181cm^{-1} , previously assigned as a deformation mode, may overlap a thallium aBR mode. The strongly covalent modes of thallium, which comprises a total of only 5 atom % of the sample, are not expected to be strong in the infrared.

Since virtually all of the thallium at aBR sites is observed crystallographically²⁰ to occupy positions displaced slightly from the aBR position, the symmetry is lowered and we may apply selection rules for mO symmetry or even lower symmetry. In this case, the A_{1g} at 165cm^{-1} and the E_{2g} at 197cm^{-1} are primarily out-of-plane vibrational modes while the E_{1g} at 120cm^{-1} is basically an in-plane vibration. For modes at BR sites, there should likewise be a large frequency difference between in-plane and out-of-plane vibrations, so the latter occurs at 105cm^{-1} while the former occur below 60cm^{-1} .

C. Divalent Ions

In sodium β -alumina which is partially exchanged with divalent cations, we expect the population of sodium on mO sites to approach zero before a significant decrease in the BR site population occurs regardless of the site occupied by the divalent ion. Since each M^{2+} ion formally replaces two Na^+ ions, the sodium population on BR sites should initially remain constant if M^{2+} occupies BR sites and should increase slightly at low degrees of exchange if M^{2+} is stabilized at other sites. The spectroscopic evidence for this process is equivocal due to competing processes discussed below.

Calcium ion, which is nearly the same size as sodium ion,

initially lowers the population of sodium on mO sites when powdered β -alumina is exchanged in melts containing between 5 and 100 mole percent CaCl_2 at 950°C . In Figure 11, the sodium band on mO sites at 115cm^{-1} disappears as the rate of exchange increases while the BR site band at 90cm^{-1} is little affected. At the same time, a band at 150cm^{-1} grows in due to calcium ion vibrations. At the highest degree of exchange, a phase change occurs² from β -alumina to $\text{CaO}\cdot 5\text{Al}_2\text{O}_3$ resulting in a greatly altered spectrum. Two other bands in this figure at lower degrees of exchange are deformation modes involving aluminum and oxygen.

The lower frequency aluminum-oxygen deformation mode at 165cm^{-1} is quite sensitive to the nature of the exchangeable cations. In β -alumina containing only monovalent cations, this band tends to appear at lower frequency with large ions such as rubidium or cesium and at higher frequency with small ions such as sodium and ammonium. In samples exchanged with strontium or lead, the band appears at 140cm^{-1} and 120cm^{-1} respectively. The ion motion bands of strontium grow in coincidentally at the deformation mode frequency and split at higher exchange levels to form a complex manifold while the ion motion bands of lead grow in at 70cm^{-1} and 130cm^{-1} . Overlapping bands at the mO Na frequency shown in Figures 12 and 13 preclude hard data in support of sodium on mO sites being replaced first.

Exchange of sodium with the small ions, Mn^{2+} , Fe^{2+} , Co^{2+} , or Ni^{2+} , however, also shifts the deformation mode to low frequency, about $130cm^{-1}$. The spectra of these samples prepared from melts containing less than 50 mole % metal chloride are nearly identical as shown in Figure 14 and summarized in Table V. The intensity and shape of the band near $130cm^{-1}$ is nearly invariant with increasing degree of exchange in all samples arising from melts containing 5-50mole percent transition metal ion. Below $500cm^{-1}$, the only other significant change in these spectra relative to sodium β -alumina is the broadening of the band near $80cm^{-1}$ and the shift of this band to lower frequency. Crystal fracture due to lattice strain becomes evident in samples from melts containing over 50mole % transition metal. The smearing of spectral features at high exchange arises from the nature of finely pulverized samples and chemisorbed water present.³¹

Since the transition metal ions are small they achieve closer ionic coordination in the chloride melt than in the solid β -alumina, and Yao and Kummer² were able to incorporate only 0.45mole of divalent metal (corresponding to 33% Na exchange). The broad, low frequency band, therefore, will have a persistent contribution from residual sodium at all exchange levels, but this band will be augmented in intensity by the transition metal vibrational modes. Unlike strontium and lead which must expand the lattice, these divalent ions are not sterically constrained

so the effects of increased mass and charge relative to sodium will nearly counterbalance each other to produce a vibrational frequency of about 70cm^{-1} .

Determination of cation sites occupied in transition metal substituted β -alumina is complicated by the fact that possible sites are not only those within the conduction plane but also aluminum sites within the spinel block. Fe^{2+} , Ni^{2+} , Cu^{2+} , and Zn^{2+} as well as Mg^{2+} have been found to substitute isomorphically for aluminum in β -alumina^{26,32} when sintered at 1500°C . At much lower temperatures (700°C), electron paramagnetic resonance studies³³ indicate the Cu^{2+} and Mn^{2+} substituted by molten salt exchange for Na^{+} migrate easily in the spinel blocks and tend to occupy tetrahedral sites.

Although Collongues et al.³³ found by epr that Cu^{2+} and Mn^{2+} occupy several non-equivalent sites within the conduction plane, the presence of only a single low frequency band in our infrared results for various transition metals suggests that, energetically, these sites are nearly equivalent. Under our conditions of exchange ($\sim 950^{\circ}\text{C}$), equilibrium will favor trivalent aluminum within the close-packed oxygen layers of the spinel block rather than in the chloride melt; therefore, replacement of Al^{3+} with M^{2+} will not increase the mobile ion concentration in the conducting planes as in high temperature sintering.³² Furthermore, the presence of a low concentration of transition metal in the spinel block will be insufficient to create any new observable

infrared bands because of rigid coupling within the blocks but may account for the low frequency shift of the lattice mode near 130cm^{-1} .

Probable transition metal sites include interstitial positions above and below the mid-oxygen sites of the conduction plane. Interstitial aluminum was discovered¹⁵ at these sites by neutron diffraction and presumably is coordinated tetrahedrally to interstitial oxygen on the mid-oxygen sites. In cobalt and nickel exchanged samples, the visible spectra shown in Figure 15 change only in the intensity of blue reflected as the transition metal content increases. In tetrahedral coordination, the bands shown correspond to ${}^4T_1(P) + {}^4A_2(F)$ for cobalt and ${}^3T_1(P) + {}^3T_1(F)$ for nickel with $10Dq$ values in the range $4000\text{-}5000\text{cm}^{-1}$. This is in the range expected for oxygen ligands, and the band structure is typical of that arising from spin-orbit coupling in tetrahedral complexes of these ions.³⁴

CONCLUSIONS

Beta-alumina containing various mobile monovalent ions exhibits a richly structured spectrum in the far-infrared. By observing changes in the spectrum as the cation content is altered, we have been able to assign many of the observed bands to ions occupying specific sites and vibrating either parallel with or perpendicular to the conducting planes. Ionic vibrational bands have also been observed for β -alumina substituted with divalent ions and spectra corresponding to solid state phase changes have been noted.

ACKNOWLEDGMENTS

This research was supported in part by the Office of Naval Research of the U. S. Navy. We gratefully acknowledge the support and use of Central Facilities of the Material Research Laboratory of Brown University supported by the National Science Foundation.

REFERENCES

1. W. Van Gool. ed., "Fast Ion Transport in Solids, Solid State Batteries and Devices", North Holland, Amsterdam, 1973.
2. Y.F.Y. Yao and J. T. Kummer, J. Inorg. Nucl. Chem. 29, 2453 (1957).
3. G. J. Exarhos and W. M. Risen, Jr., Sol. St. Commun. 11, 755 (1972).
4. R. D. Armstrong, P.M.A. Sherwood, and R. A. Wiggins, Spectrochim. Acta 30A, 1213 (1974).
5. L. L. Chase, C. H. Hao, and G. D. Mahan, Sol. St. Commun. 18, 401 (1976).
6. M. J. Rice and W. L. Roth, J. Solid State Chem. 4, 294 (1972).
7. G. J. Exarhos, P. JH. Miller, and W. M. Risen, Jr., Solid St. Commun. 17, 29 (1975).
8. S. J. Allen and J. P. Remeika, Phys. Rev. Lett. 33, 1478 (1974).
9. B. A. Huberman and P. N. Sen, Phys. Rev. Lett. 33, 1379 (1974).
10. H. Sato and R. Kikuchi, J. Chem. Phys. 55, 677 (1971).
11. a. W. Van Gool, J. Solid State Chem. 7, 55 (1973); b. W. Van Gool and P. H. Bottleberghs, J. Solid State Chem. 7 59 (1973).
12. J. C. Wang, M. Gaffari, and S. Choi, J. Chem. Phys. 63, 772 (1975).
13. C. A. Beevers and M.A.S. Ross, Z. Kristallogr. 95, 472 (1936).
14. R. C. DeVries and W. L. Roth, J. Am. Ceram. Soc. 52, 364 (1969).

15. W. L. Roth, F. Reidinger, and S. J. LaPlace, Conference on Superionic Conductors, Schenectady, New York, May 1976.
16. M. S. Whittingham and R. A. Huggins, *J. Electrochem. Soc.* 118, 1 (1971).
17. C. R. Peters, M. Bettman, J. W. Moore, and M. D. Glick, *Acta Cryst.* B27, 1826 (1971).
18. P. D. Dernier and J. P. Remeika, *J. Solid State Chem.* 17, 245 (1976).
19. W. L. Roth, *J. Solid State Chem.* 4, 60 (1972).
20. T. Kodama and G. Muto, *J. Solid State Chem.* 17, 61 (1976).
21. Y. Le Cars, R. Comes, L. Deschamps, and J. They, *Acta Cryst.* A30, 305 (1974).
22. D. B. McWhan, P. D. Dernier, C. Vettier, and J. P. Remeika, Conference on Superionic Conductors, Schenectady, New York, May 1976.
23. I. Chung, H. S. Story, and W. L. Roth, *J. Chem. Phys.* 57, 5180 (1972).
24. J. P. Boilot, L. Zuppiroli, G. Delplanque, and L. Jerome, *Phil. Mag.* 32, 343 (1975).
25. M. Harata, *Mat. Res. Bull.* 6, 461 (1971).
26. A. Imai and M. Harata, *Japan. J. Appl. Phys.* 11, 180 (1972).
27. N. Weber and A. Venero, 72nd Annual Meeting of Am. Ceram. Soc., May 1970.
28. J. H. Kennedy and A. F. Sammells, *J. Electrochem. Soc.* 119, 1609 (1972).
29. R. H. Radzilowski and J. T. Kummer, *J. Electrochem. Soc.* 118, 714 (1971).

30. U. Strom, P. C. Taylor, S. G. Bishop, T. L. Reinecke,
and K. L. Ngai, Phys. Rev. B13, 3329 (1976).
31. J. R. Tessman, A. H. Kahn, and W. Shockley, Phys. Rev.
92, 890 (1953).
32. J. H. Kennedy and A. F. Sammells, J. Electrochem. Soc.
121, 1 (1974).
33. R. Collongues et al., Conference on Superionic Conductors,
Schenectady, New York, May 1976.
34. B. N. Figgis, "Introduction to Ligand Fields", Wiley,
New York 1966.

TABLE I

Cation Site Occupation Parameters at Room Temperature

Ion	Site Occupancy / Unit Cell			ref
	BR	m0	aBR	
Na	1.50	1.04	0.0	17
K	1.42	1.22	0.0	18
Ag	1.34	0.34	0.87	19
Tl	1.86	0.0	0.80	20

TABLE II

Symmetries of Ion Vibrations in β -Alumina

Beevers-Ross or anti-BR Sites

(2 sites / unit cell)

selection rules	D_{3h} Site symmetry	D_{6h} factor symmetry	selection rules
$\left. \begin{matrix} \alpha_{xx-yy, xy} \\ T_{x,y} \end{matrix} \right\}$	2 E'	E_{2g} E_{1u} $\alpha_{xx-yy, xy}$ $T_{x,y}$
T_z	2 A''	B_{2g} A_{2u} T_z

Mid-Oxygen Sites

(6 sites / unit cell)

selection rules	C_{2v} site symmetry	D_{6h} factor symmetry	selection rules
$\left. \begin{matrix} \alpha_{xx}, \alpha_{yy}, \alpha_{zz} \\ T_z \end{matrix} \right\}$	6 A_1	A_{1g} A_{2u} E_{2g} E_{2u} $\alpha_{xx} + yy, \alpha_{zz}$ T_z $\alpha_{xx-yy, xy}$
$\left. \begin{matrix} \alpha_{xz} \\ T_x \end{matrix} \right\}$	6 B_1	B_{1g} B_{2u} 2 E_{1g} 2 E_{1u} $\alpha_{xz, yz}$ $T_{x,y}$
$\left. \begin{matrix} \alpha_{yz} \\ T_y \end{matrix} \right\}$	6 B_2	B_{2g} B_{1u}	

TABLE III
Observed Far-Infrared Bands and Assignments
for Monovalent β -alumina

NH_4^+			
(cm^{-1})	intens	symmetry	origin
151	ms	--	BR
194	m	E_{1u}	Al-O def
233	ms	E_{1u}	Al-O def
Na^+			
(cm^{-1})	intens	symmetry	origin
55	w, sh	E_{1u}	BR
87	s	A_{2u}	BR
113	m	--	mO
167	m	E_{1u}	Al-O def
213	ms	E_{1u}	Al-O def
K^+			
(cm^{-1})	intens	symmetry	origin
53	w, sh	--	--
72	wm	--	mO
87	m	A_{2u}, E_{1u}	BR
109	wm	--	mO
183	ms	E_{1u}	Al-O def
223	s	E_{1u}	Al-O def

TABLE III(con't)

Rb^+			
ν (cm^{-1})	intens	symmetry	origin
28	w	--	--
39	w	--	--
49	w, sh	--	--
69	wm	--	mO
82	m	--	BR
167	m	E_{lu}	Al-O def
232	s	E_{lu}	Al-O def

Cs^+			
ν (cm^{-1})	intens	symmetry	origin
27	w, sh	--	Ag?
47	w, sh	--	--
74	s	--	BR
112	wm	--	Ag
148	ms	E_{lu}	Al-O def
239	s	E_{lu}	Al-O def

Ag^+			
ν (cm^{-1})	intens	symmetry	origin
38	s	E_{lu}	BR
74	ms	E_{lu}	aBR
84	m	--	mO
112	ms	--	aBR
161	ms	E_{lu}	Al-O def
210	ms	E_{lu}	Al-O def

TABLE III(con't)

Tl⁺

ν (cm ⁻¹)	intens	symmetry	origin
31	wm	--	(BR)
48	vs	E _{1u}	BR
60	m, sh	--	(BR)
97	vs	A _{2u}	BR
181	ms	E _{1u}	Al-O def, aBR
224	s	E _{1u}	Al-O def

TABLE IV

Assignments and Relative Intensities of How Frequency
Raman Bands in β -Aluminas^a

Na^+						
ν (cm^{-1})	symmetry	origin	rel. intens. $x(yy)z$ $x(yx)z$		rel. intens. $x(zz)y$ $x(zx)y$	
60	E_{2g}	BR	off	m	off	off
84	A_{1g}	lattice	35	8	19	4
99	E_{2g}	m0	45	40	6	6
113	E_{1g}	m0	3	2	10	35
256	A_{1g}	Al-O def	100	12	100	11
K^+						
ν (cm^{-1})	symmetry	origin	rel. intens. $x(yy)z$ $x(yx)z$		rel. intens. $x(zz)y$ $x(zx)y$	
69	E_{2g}	BR	7	7	—	2
83	A_{1g}	lattice	12	13	26	7
96	E_{2g}	m0	6	9	1	3
120	E_{1g}	m0	2	4	17	29
260	A_{1g}	Al-O def	100	10	100	17
Ag^+						
ν (cm^{-1})	symmetry	origin	rel. intens. $x(yy)z$ $x(yx)z$		rel. intens. $x(zz)y$ $x(zx)y$	
24	E_{2g}	BR	off	s	off	off
83	A_{1g}	lattice	26	7	52	15
103	E_{2g}	aBR	47	54	w, sh	w, sh
111	E_{1g}	aBR	11	16	140	290
258	A_{1g}	Al-O def	100	16	100	33

TABLE IV (cont'd)

 Tl^+

ν (cm^{-1})	symmetry	origin	rel. intens.		rel. intens.	
			x(yy)z	x(yx)z	x(zz)y	z(zx)y
27	--	(BR)	off	s	off	off
38	E_{2g}	BR	400	500	?	s
58	E_{1g}	(BR)	100	85	84	210
84	A_{1g}	lattice	42	23	30	19
105	E_{2g}	BR	220	230	11	23
120	E_{1g}	aBR	75	98	31	63
165	A_{1g}	aBR	62	13	w	w
197	E_{2g}	aBR	120	110	7	16
264	A_{1g}	A_{1g} -0 def	100	9	100	19

^aIntensities are relative to the A_{1g} A_{1g} -0 def mode near 260 cm^{-1} .

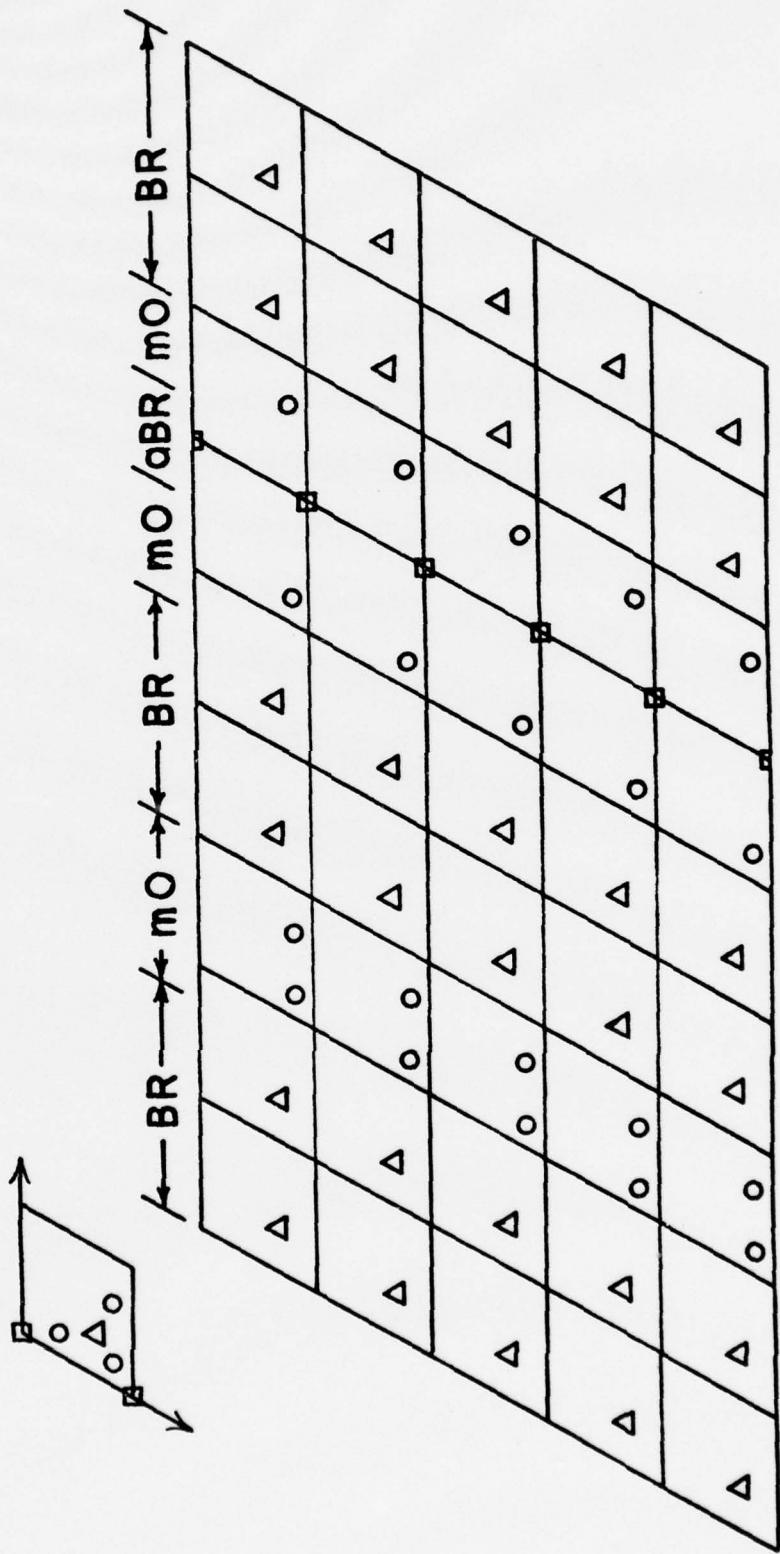
TABLE V
Far IR Bands of β -Alumina from Melts
of Composition $0.8\text{NaCl} + 0.2\text{MCl}_2$

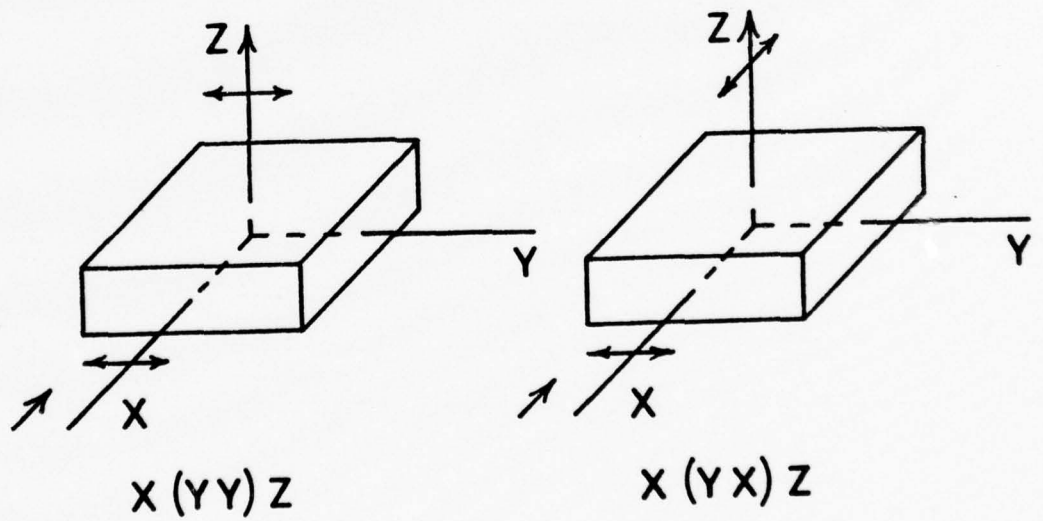
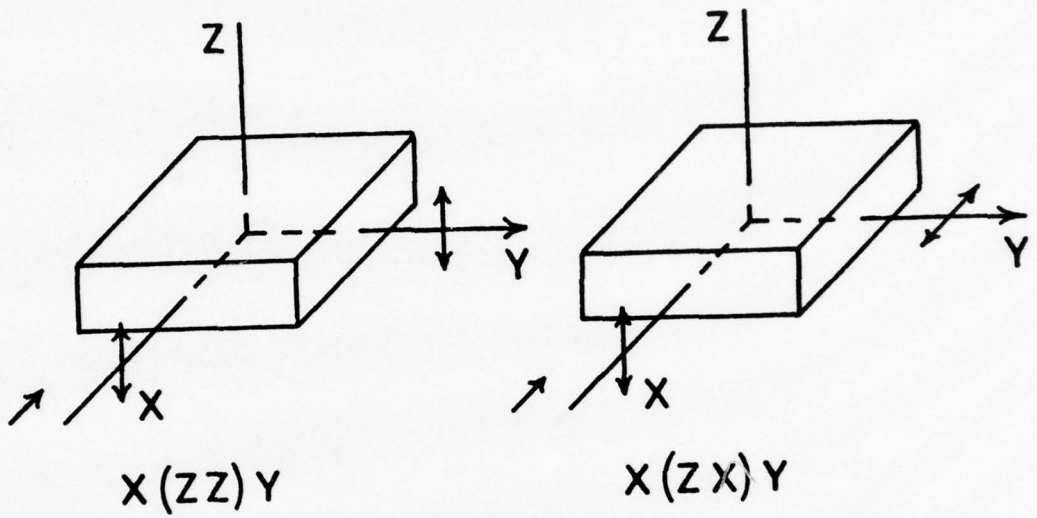
M	ν Na	ν M	ν M	δ Al-O	δ Al-O
Ca	88 m	147 s		165 m	218 s
Sr	80 v br	93 vw	136 sh	147 s	218 s
Pb		69 s	137 m	122 sh	215 s
Mn	92 sh	60 w sh		121 m	211 s
Fe	80 br	65 sh		128 m	212 s
Co	85 wm	68 sh		128 m	213 s
Ni	85 wm	66 sh		128 m	212 s

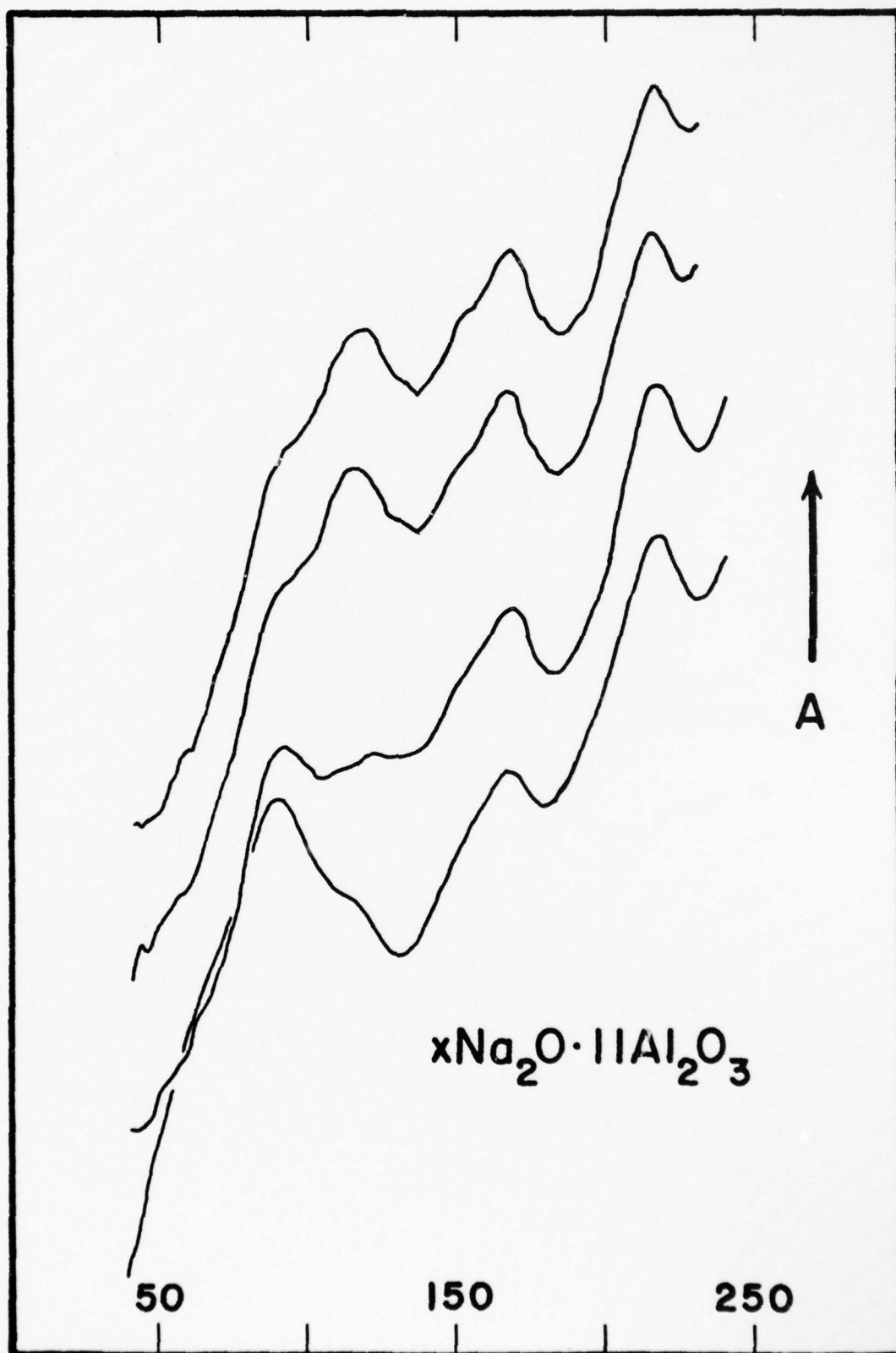
FIGURE CAPTIONS

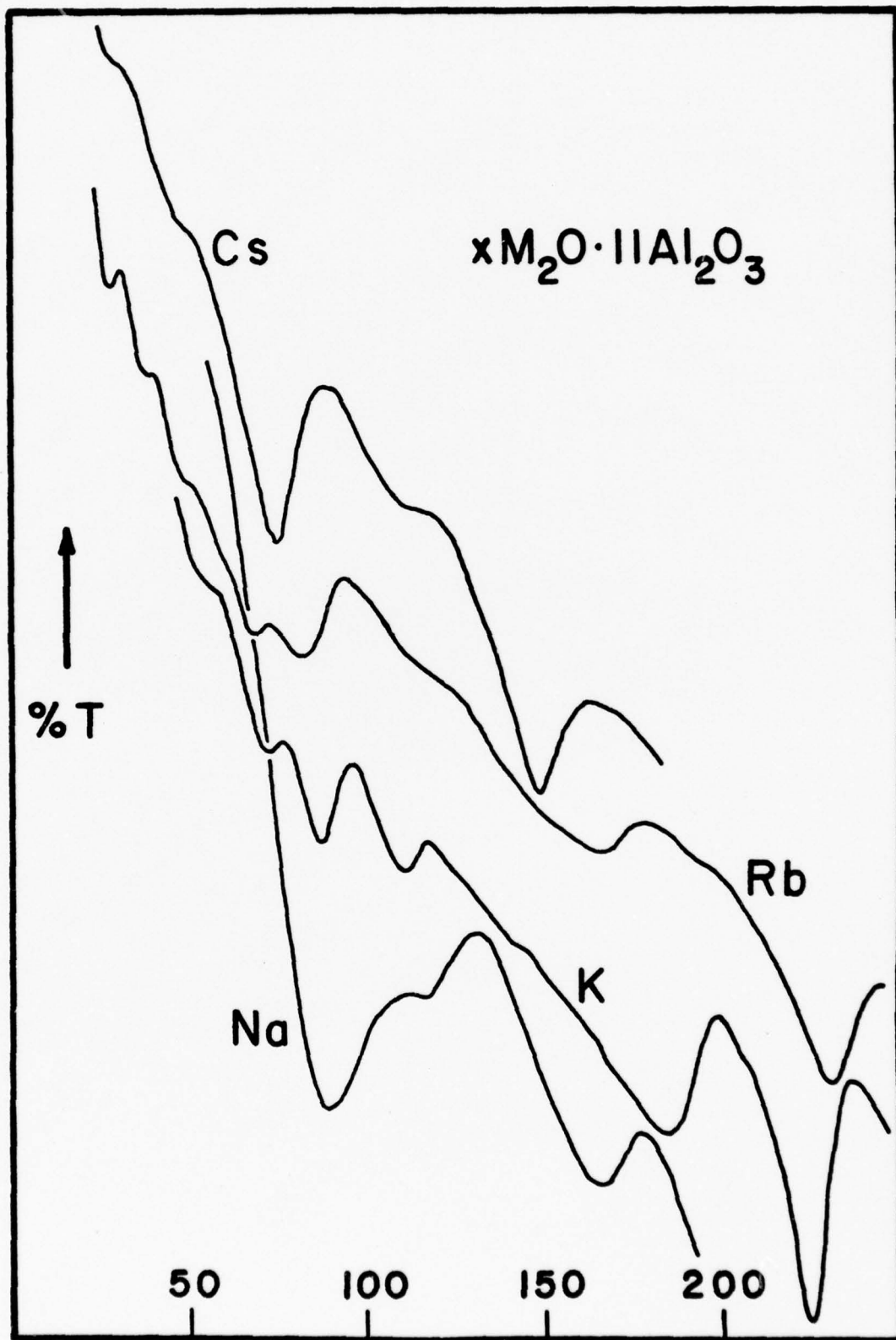
- Fig. 1. Conducting plane of β -alumina. Large solid line circles are oxygen ions; dotted circles are close packed oxygens above and below the conduction plane. Triangles are Beevers-Ross cation sites, hexagons are anti-Beevers-Ross sites, small circles are mid-oxygen sites.
- Fig. 2. The four sample orientations used for right-angle scattering geometries. The first and last letter represent the incident and scattering directions respectively. The letters in parentheses are the directions of polarization of incident and scattered light designated in the figure by a small double-headed arrow.
- Fig. 3. Far i.r. absorption spectra of Na- β -alumina with nominal stoichiometries $x = 1.2, 1.4, 1.6, \text{ and } 1.8$ from bottom to top, respectively.
- Fig. 4. Spectra of β -alumina with sodium replaced by varying amounts of potassium. Numbers on the curves do not indicate the amount of potassium exchanged but to the mole % K in the surrounding melt of $\text{KNO}_3 - \text{NaNO}_3$
- Fig. 5. Transmission spectra of Na, K, Rb, and Cs- β -alumina. The cesium sample is 50% exchanged Ag- β -alumina.
- Fig. 6. Spectra of β -alumina from nitrate melts containing the indicated mole % Ag.
- Fig. 7. Reflectance spectra from (001) face of β -aluminas with transmission spectra of powdered samples traced above: a. Na- β -alumina, b. Ag- β -alumina, c. Tl- β -alumina
- Fig. 8. Polarized Raman spectra of Na- β -alumina single crystal.

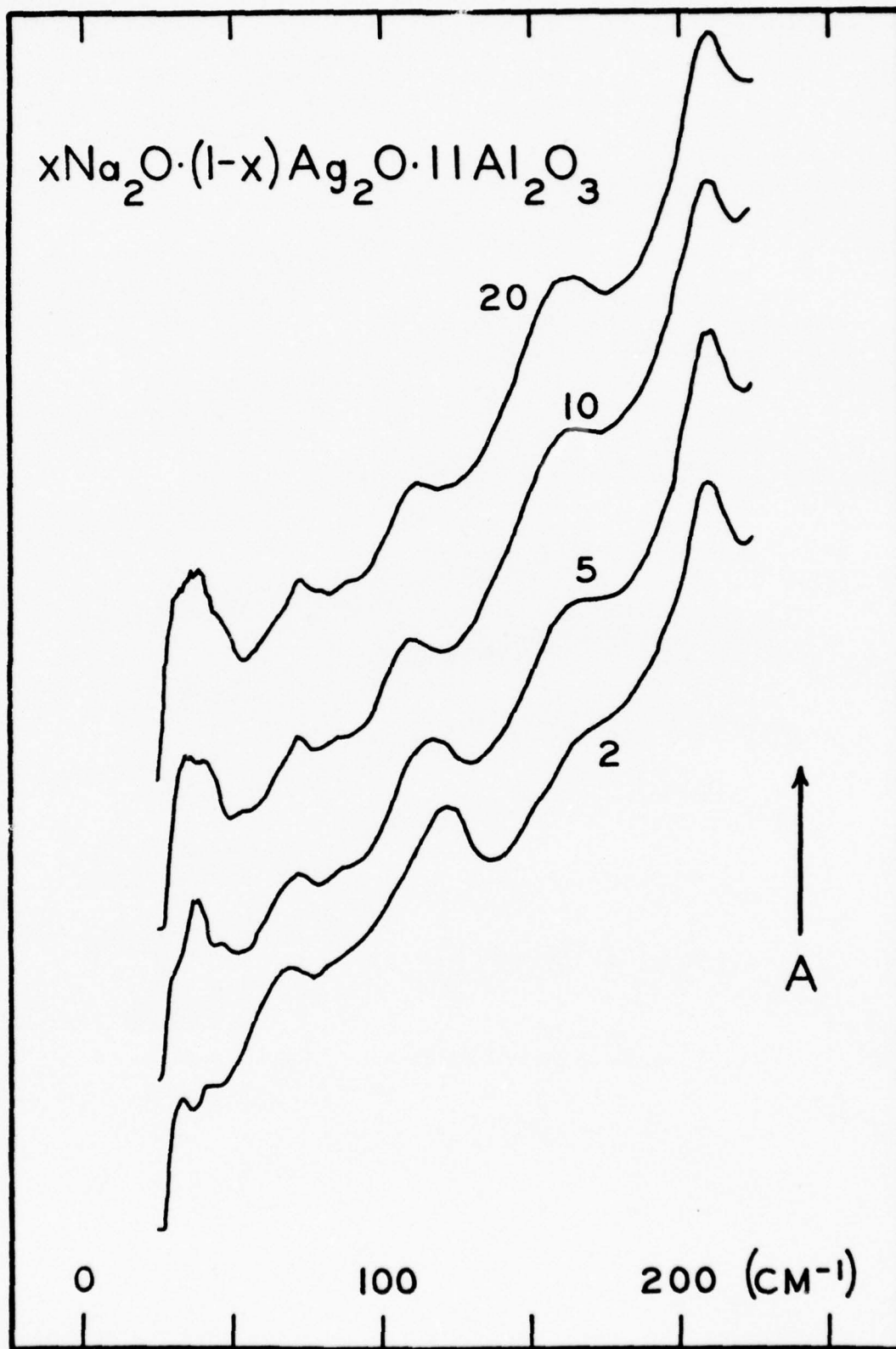
- Fig. 9. Polarized Raman spectra of Ag- β -alumina single crystal.
- Fig. 10. Polarized Raman spectra of Tl- β -alumina single crystal.
- Fig. 11. Spectra of Na- β -alumina obtained from salt melts containing between 5 and 100 mole percent CaCl_2 with the balance as NaCl.
- Fig. 12. Spectra of Na- β -alumina progressively exchanged in melts of SrCl_2 .
- Fig. 13. Spectra of Na- β -alumina progressively exchanged in melts containing the labeled mole percent PbCl_2 .
- Fig. 14. Spectra of Na- β -alumina exchanged in melts containing the labeled mole percent of Mn^{2+} , Fe^{2+} , Co^{2+} , and Ni^{2+} .
- Fig. 15. Electronic spectra of β -alumina from melts containing 50 mole % of either Ni^{2+} or Co^{2+} .

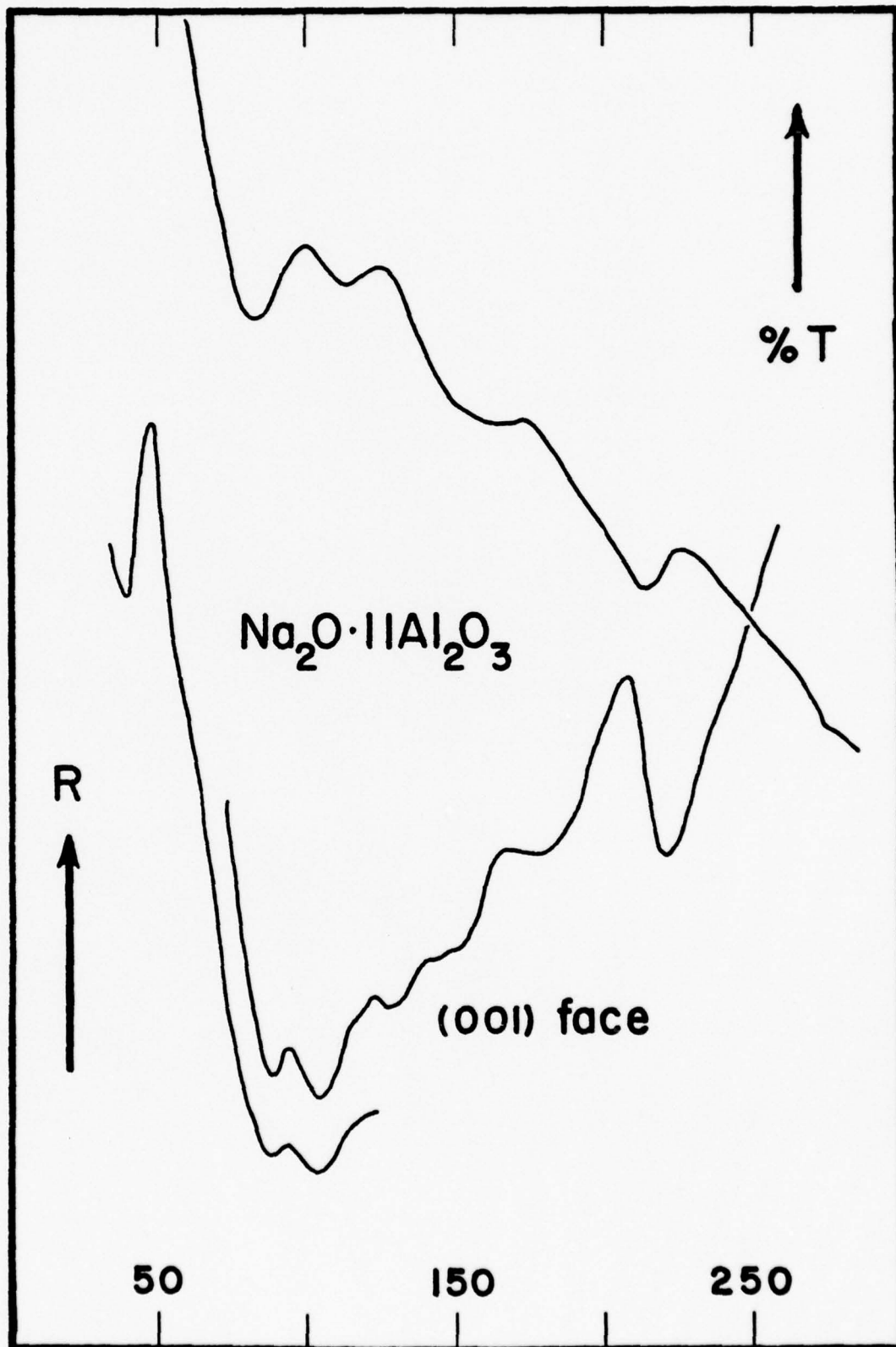


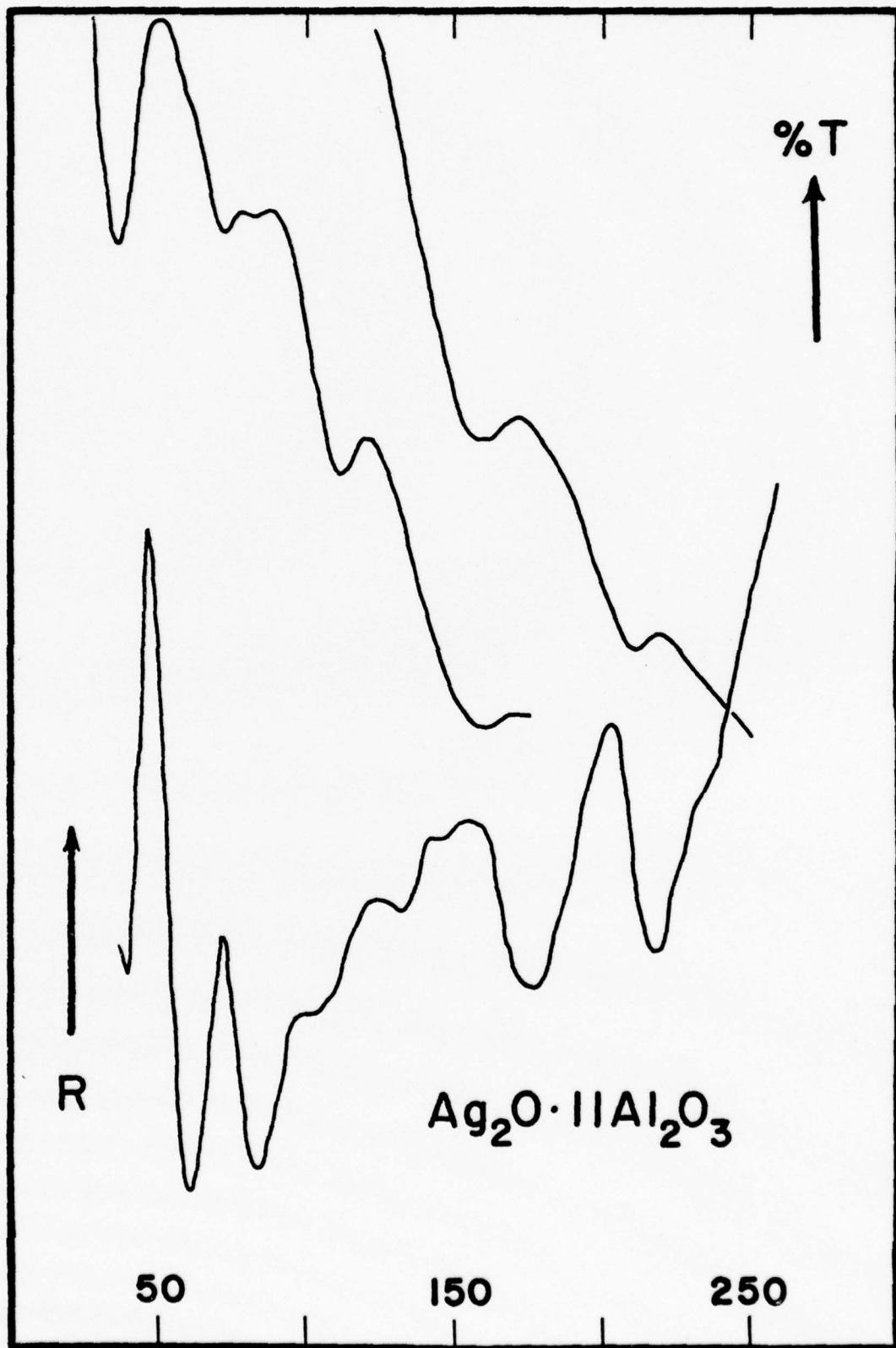


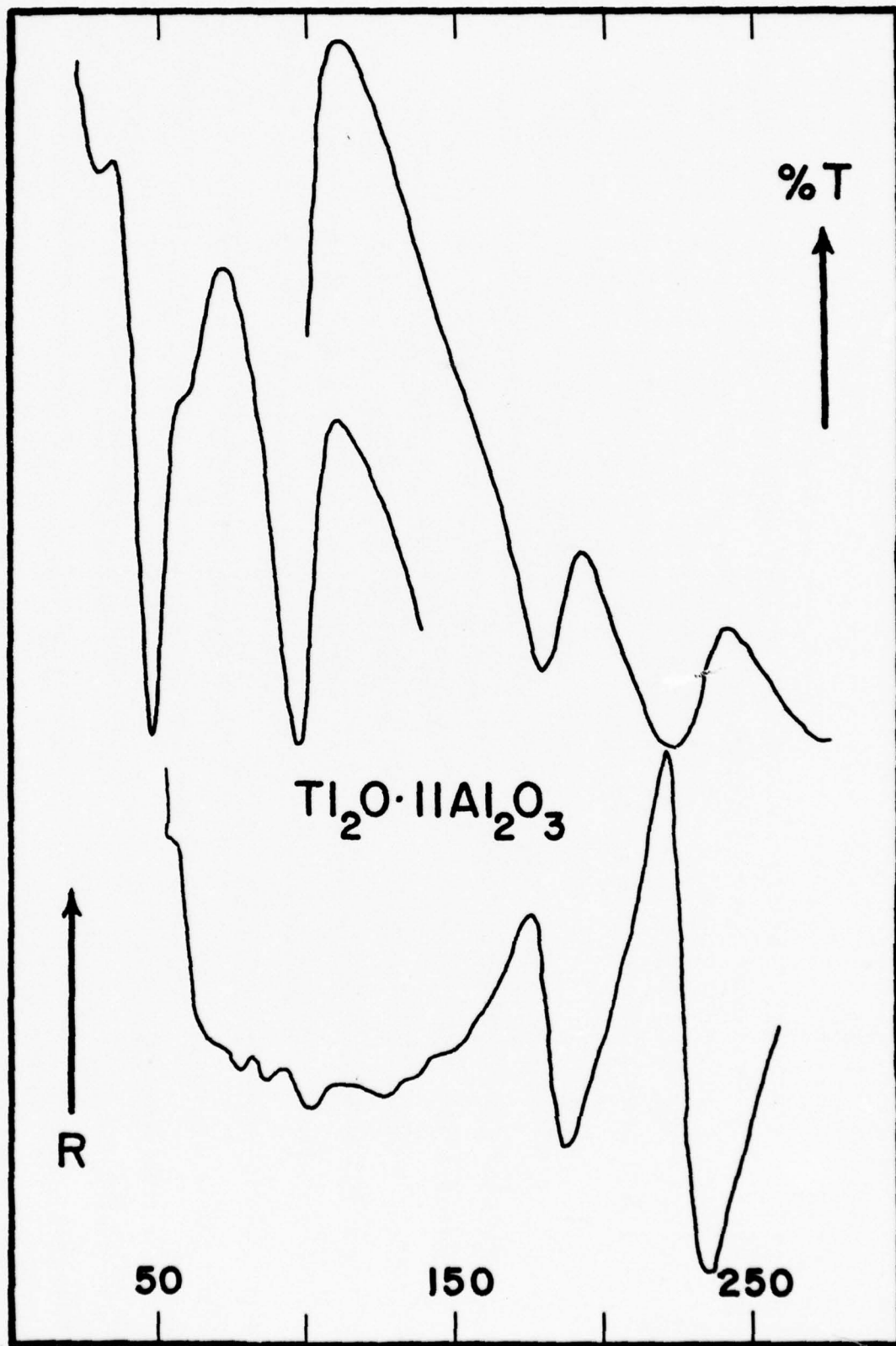


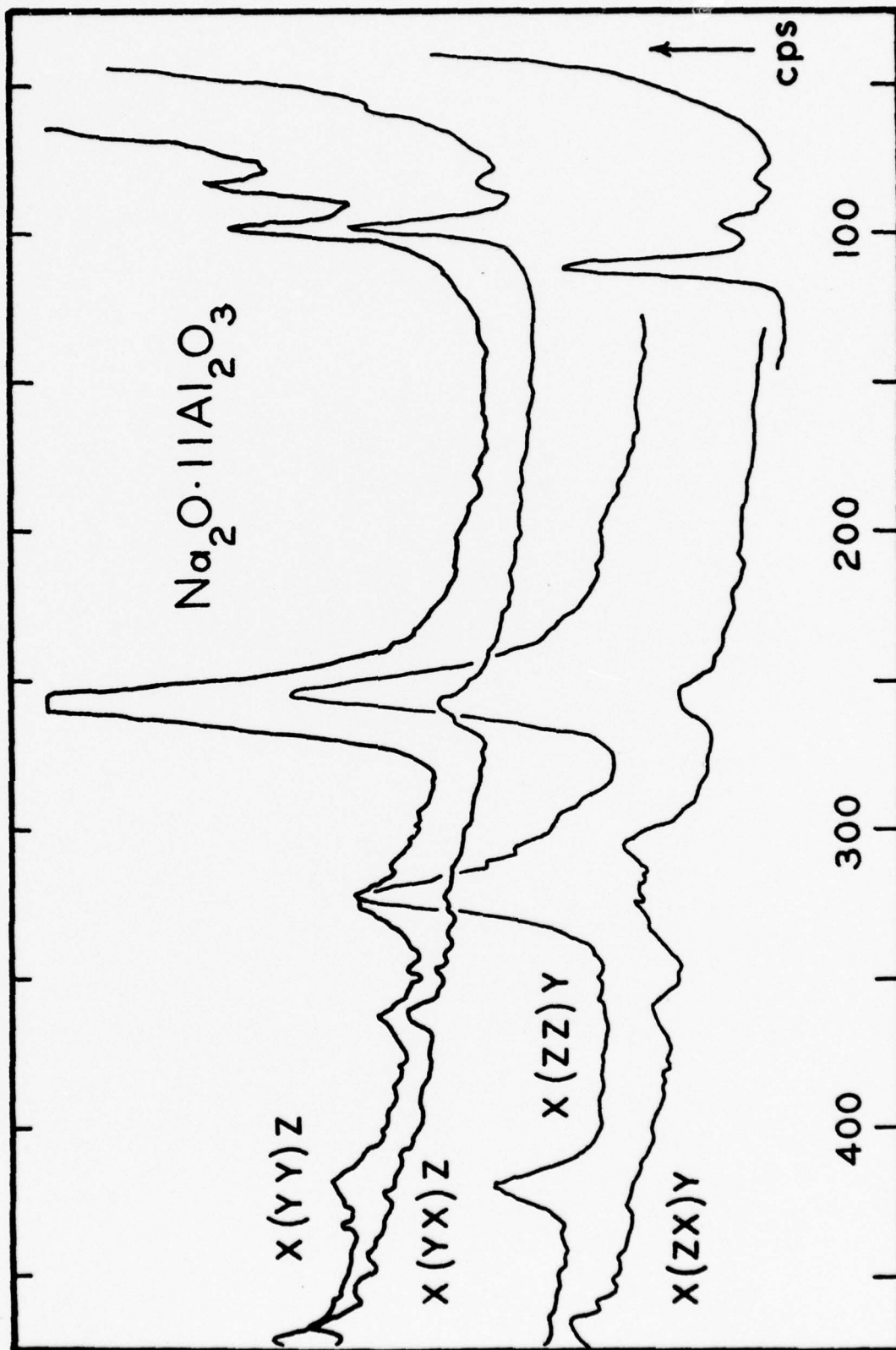


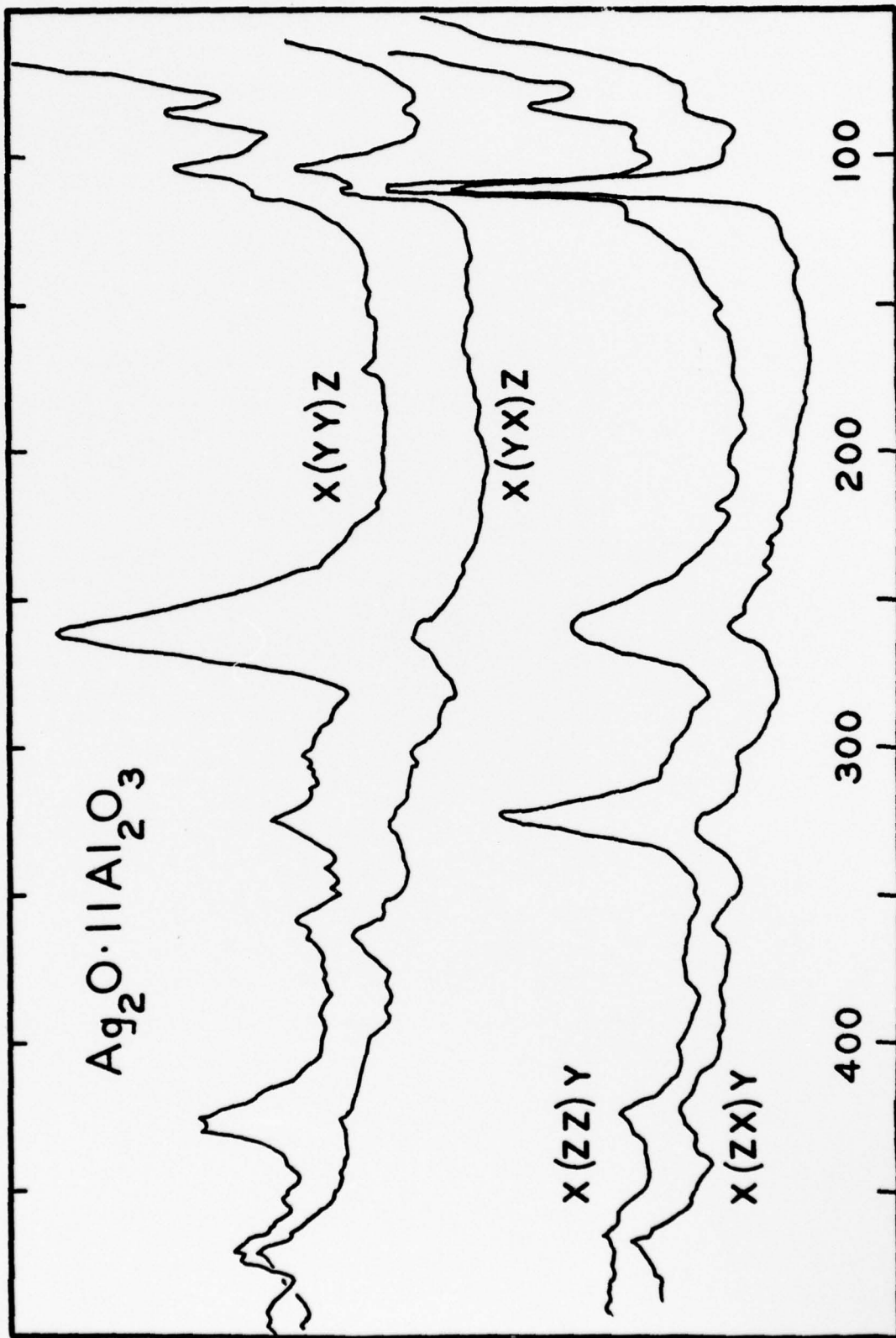


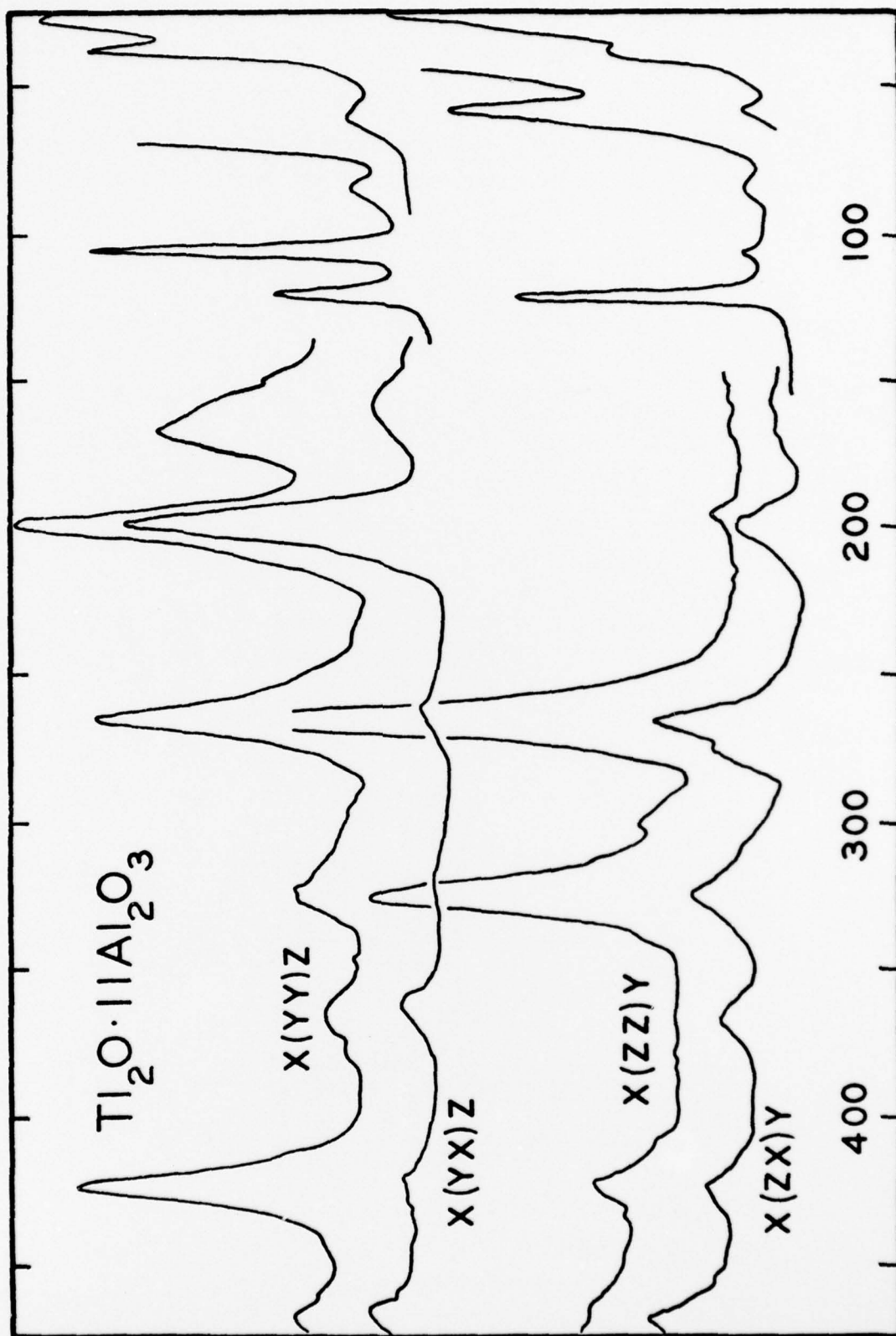


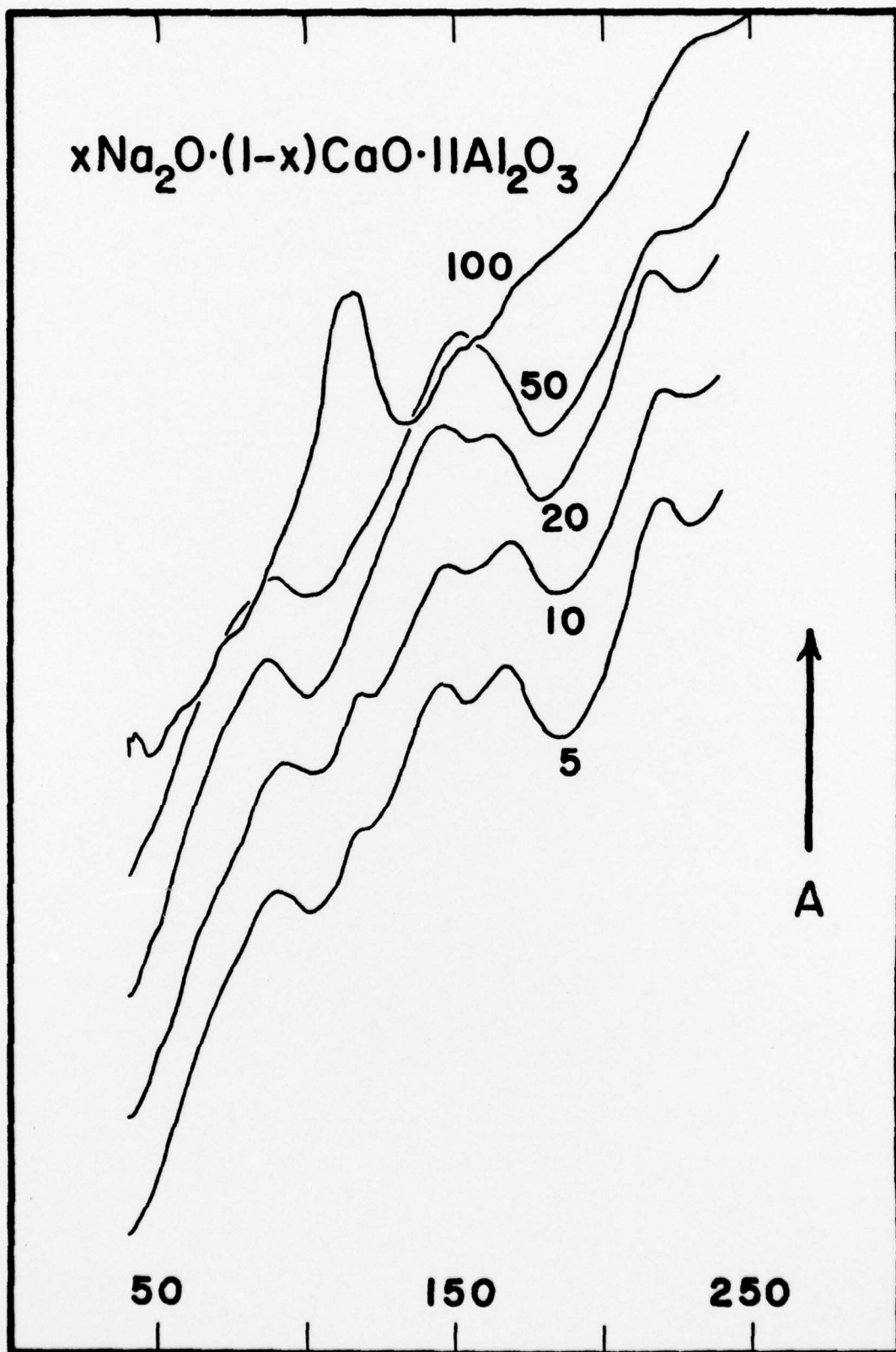


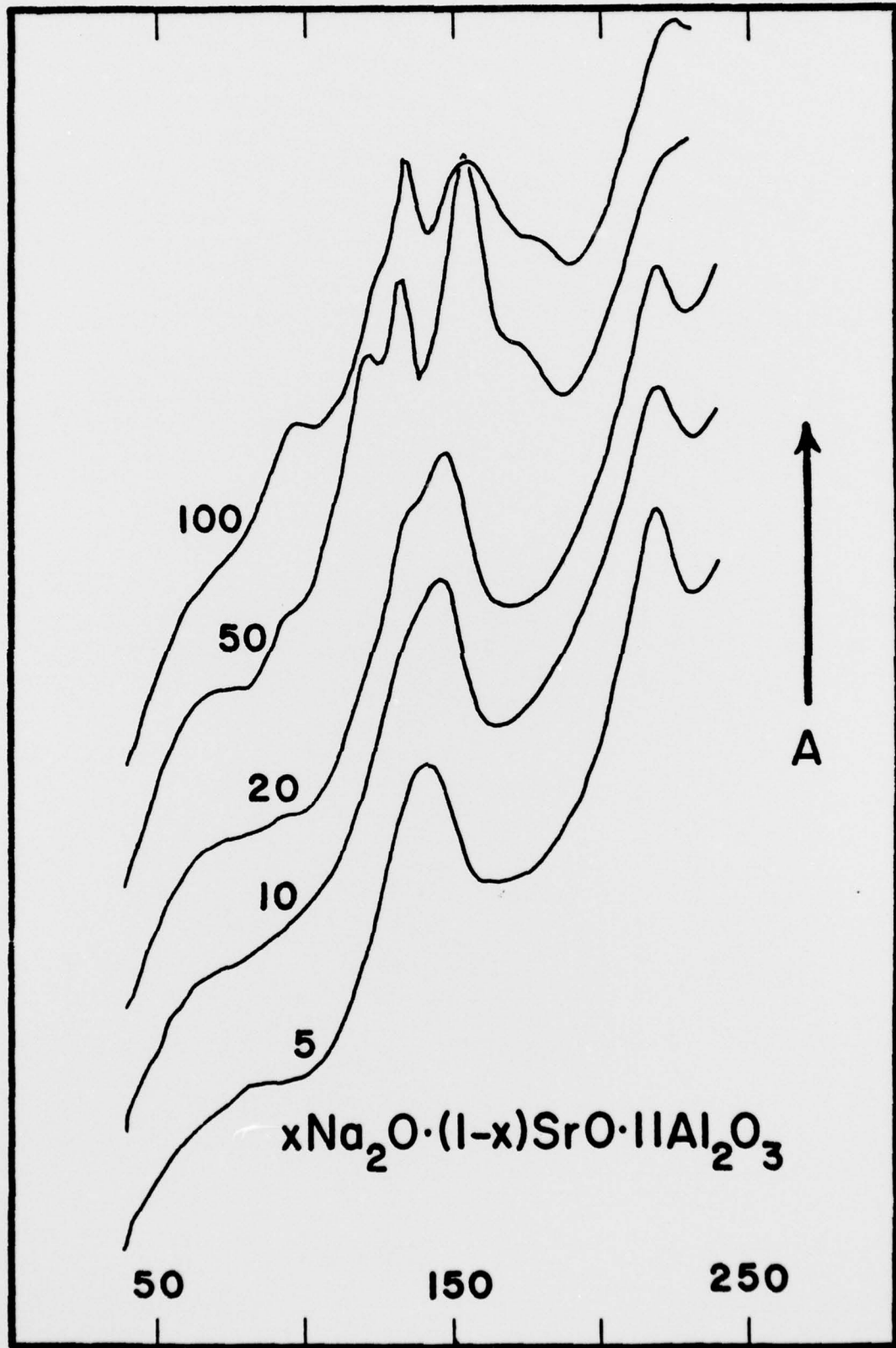


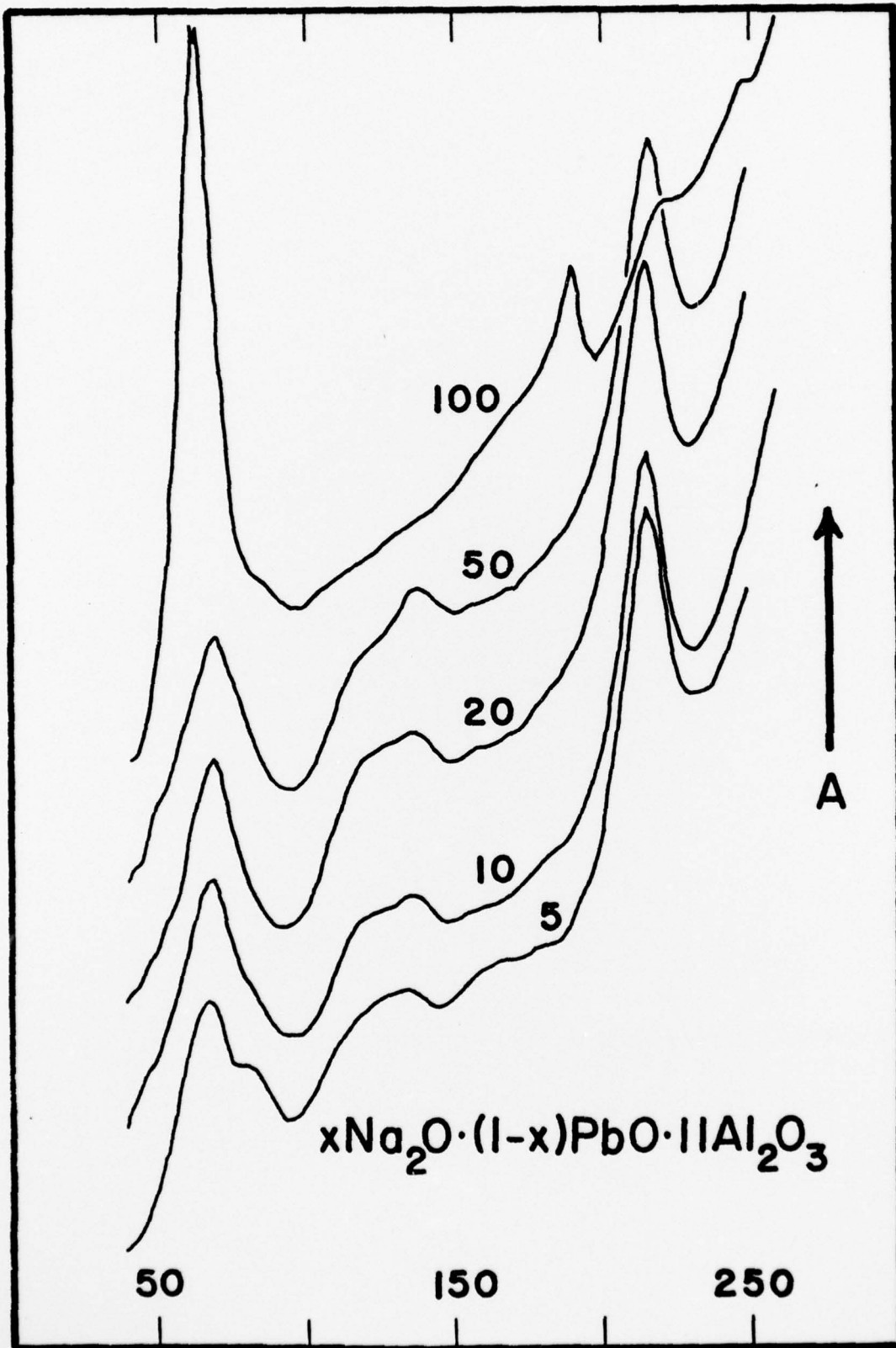


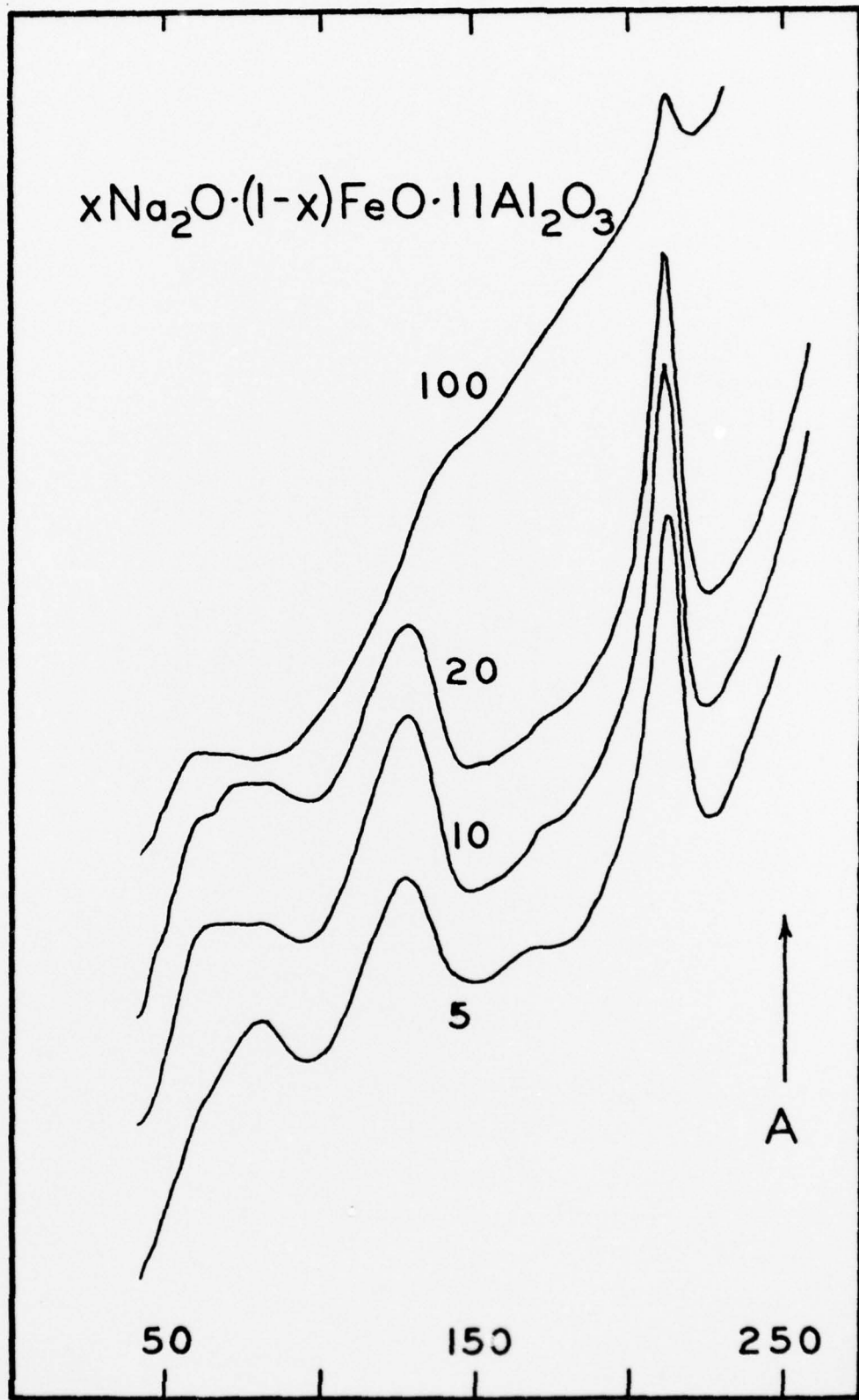


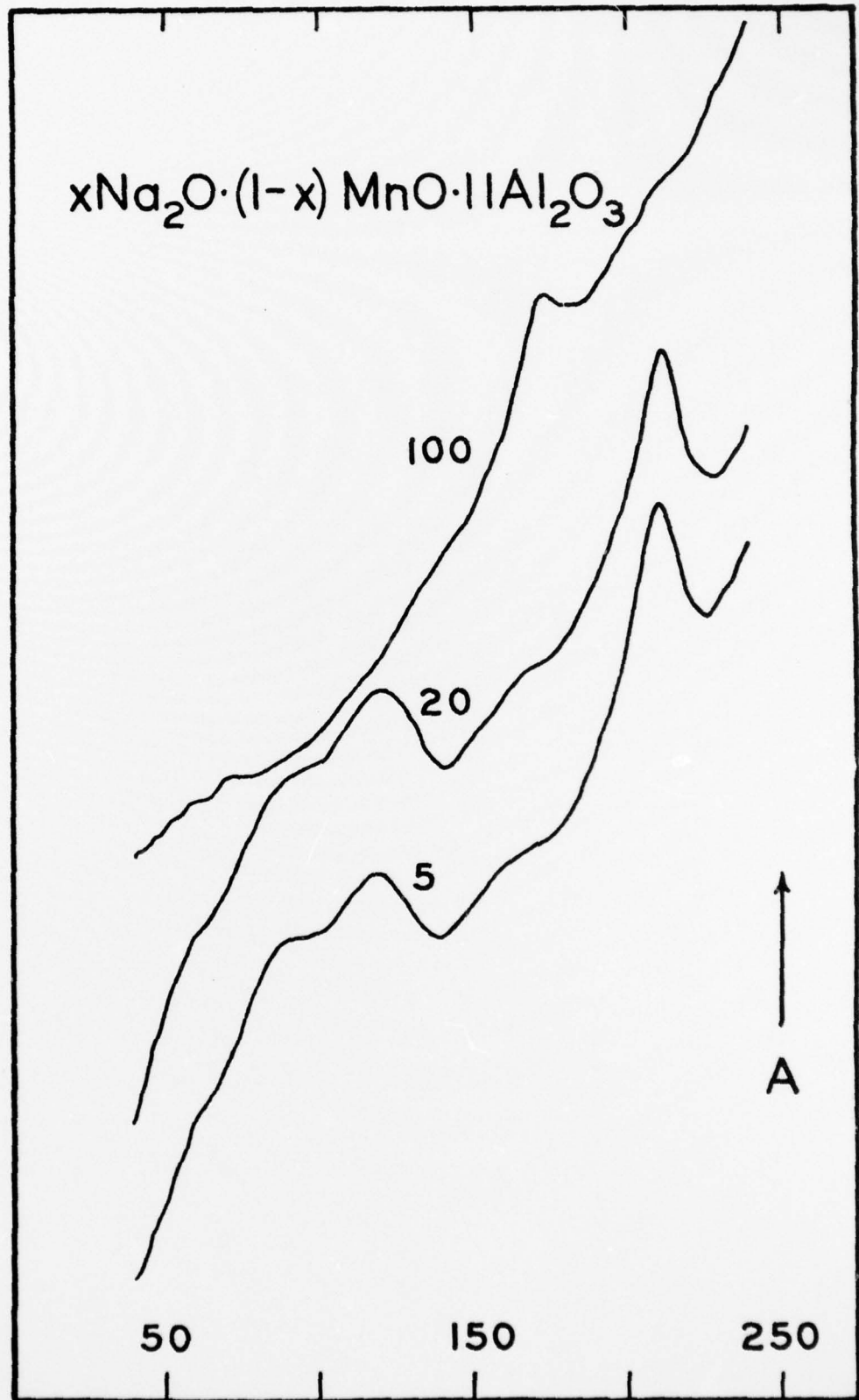


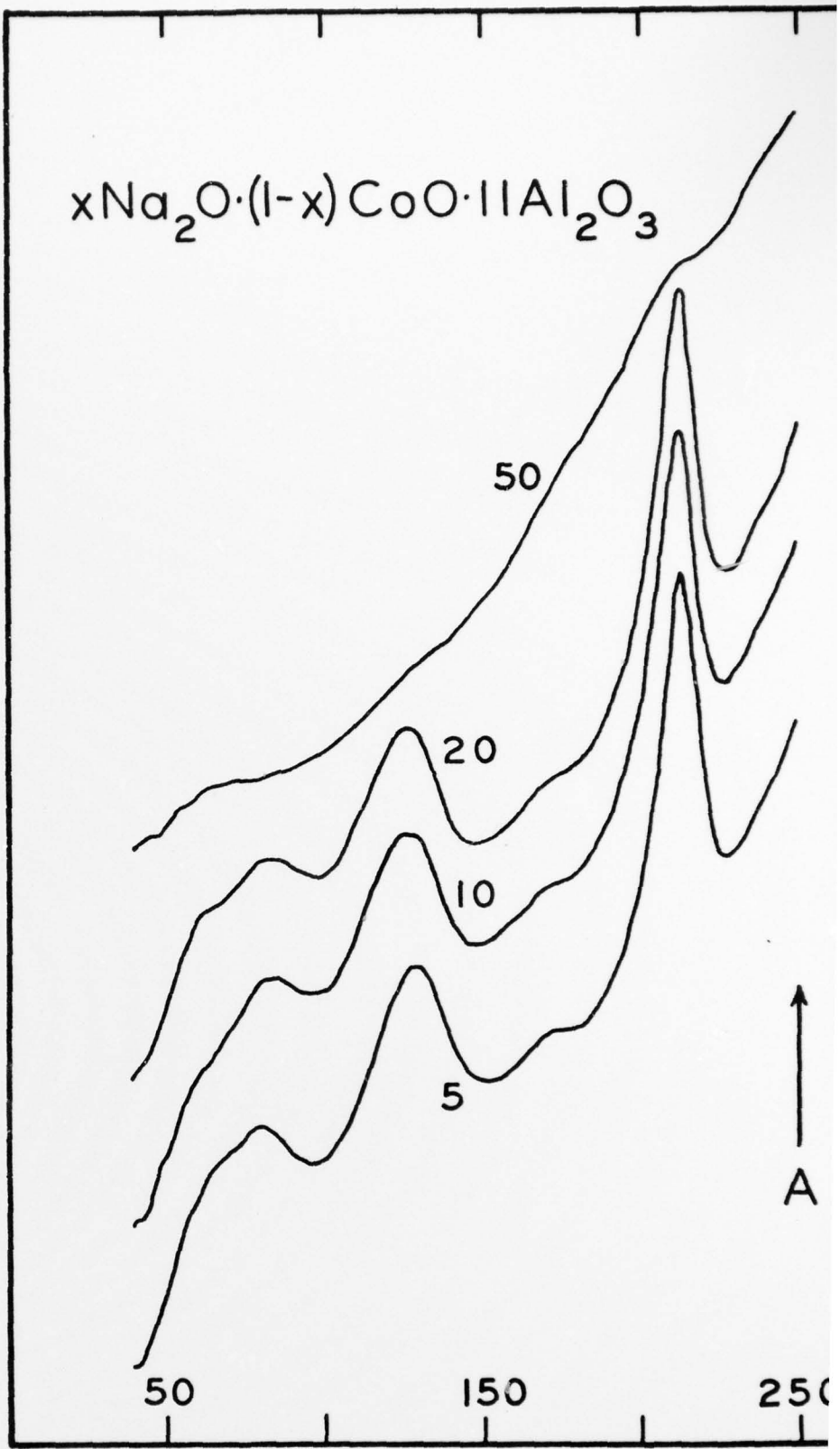
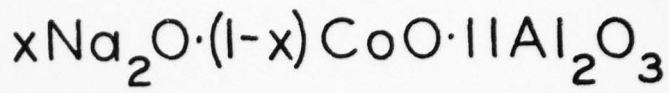


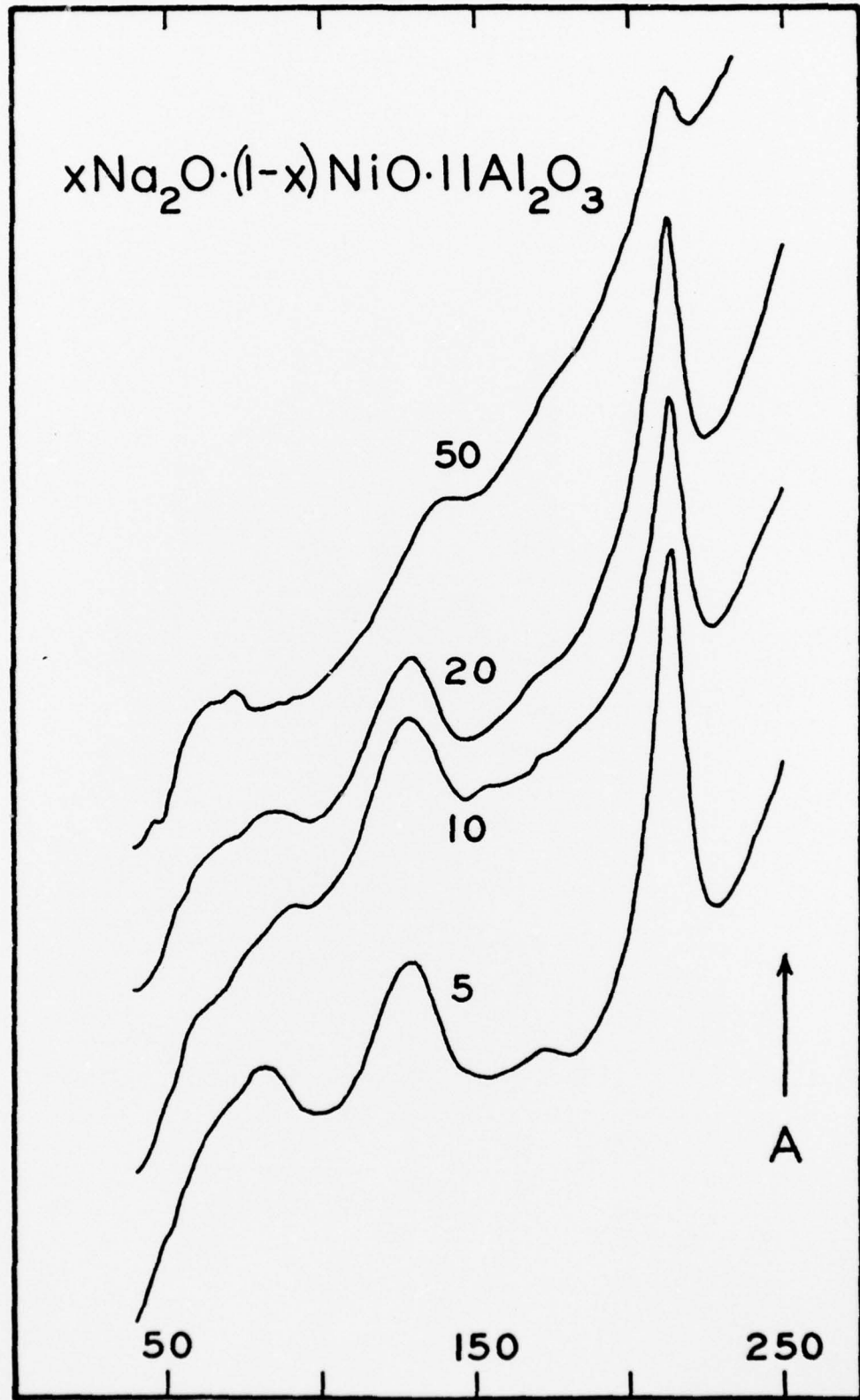


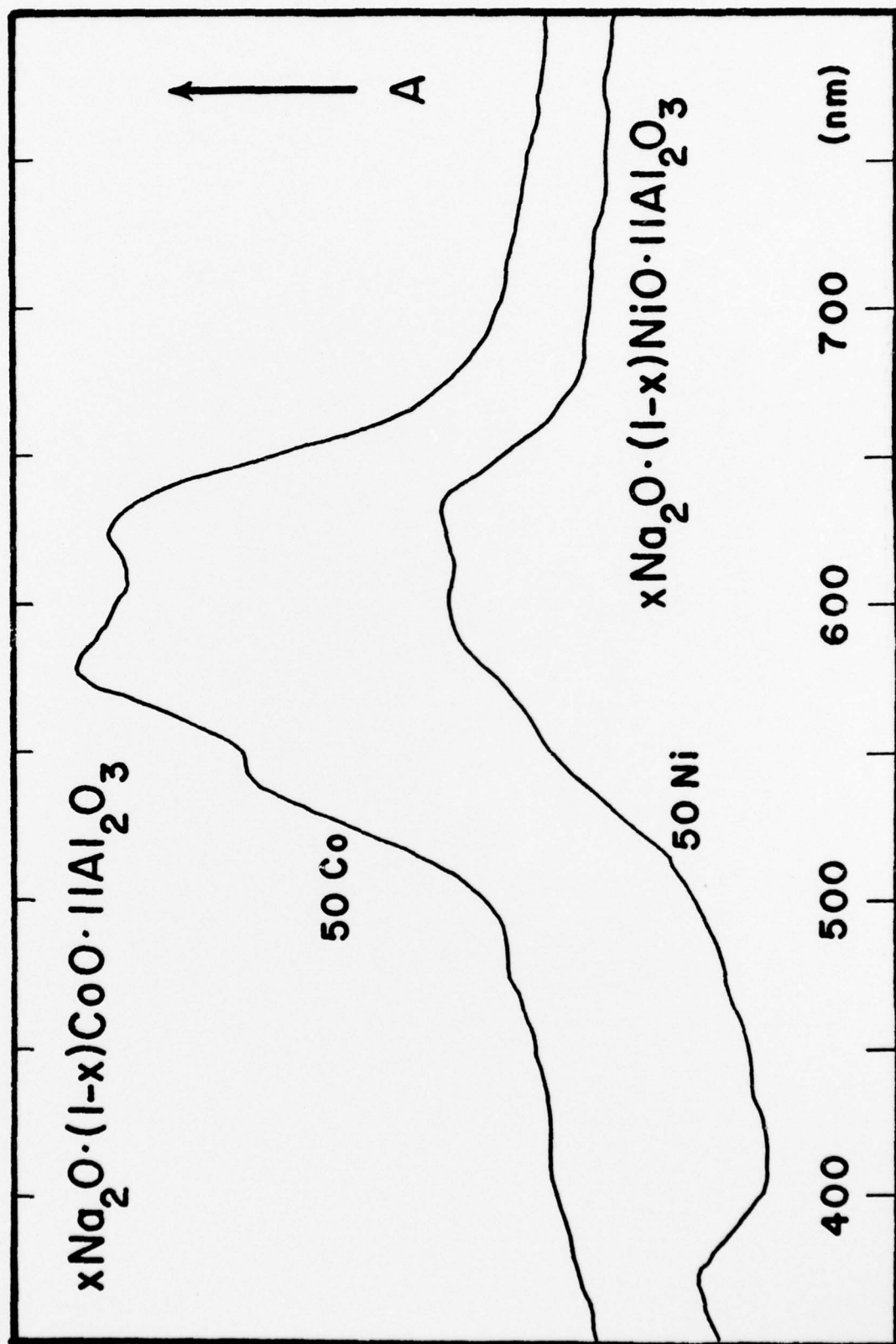












TECHNICAL REPORT DISTRIBUTION LIST

<u>No. Copies</u>		<u>No. Copies</u>
2	Office of Naval Research Arlington, Virginia 22217 Attn: Code 472	Defense Documentation Center Building 5, Cameron Station Alexandria, Virginia 22314 12
6	Office of Naval Research Arlington, Virginia 22217 Attn: Code 102IP 1	U.S. Army Research Office P.O. Box 12211 Research Triangle Park, N.C. 27709 Attn: CRD-AA-IP 1
1	ONR Branch Office 536 S. Clark Street Chicago, Illinois 60605 Attn: Dr. Jerry Smith	Naval Ocean Systems Center San Diego, California 92152 Attn: Mr. Joe McCartney 1
1	ONR Branch Office 715 Broadway New York, New York 10003 Attn: Scientific Dept.	Naval Weapons Center China Lake, California 93555 Attn: Head, Chemistry Division 1
1	ONR Branch Office 1030 East Green Street Pasadena, California 91106 Attn: Dr. R. J. Marcus	Naval Civil Engineering Laboratory Port Hueneme, California 93041 Attn: Mr. W. S. Haynes 1
1	ONR Branch Office 760 Market Street, Rm. 447 San Francisco, California 94102 Attn: Dr. P. A. Miller	Professor O. Heinz Department of Physics & Chemistry Naval Postgraduate School Monterey, California 93940 1
1	ONR Branch Office 495 Summer Street Boston, Massachusetts 02210 Attn: Dr. L. H. Peebles	Dr. A. L. Slafkosky Scientific Advisor Commandant of the Marine Corps (Code RD-1) Washington, D.C. 20380 1
1	Director, Naval Research Laboratory Washington, D.C. 20390 Attn: Code 6100	Office of Naval Research Arlington, Virginia 22217 Attn: Dr. Richard S. Miller 1
1	The Asst. Secretary of the Navy (R&D) Department of the Navy Room 4E736, Pentagon Washington, D.C. 20350	
1	Commander, Naval Air Systems Command Department of the Navy Washington, D.C. 20360 Attn: Code 310C (H. Rosenwasser)	

TECHNICAL REPORT DISTRIBUTION LIST

<u>No. Copies</u>			<u>No. Copies</u>	
	Dr. D. A. Vroom IRT P.O. Box 80817 San Diego, California 92138	1	Dr. R. W. Vaughan California Institute of Technology Division of Chemistry & Chemical Engineering Pasadena, California 91125	1
	Dr. G. A. Somorjai University of California Department of Chemistry Berkeley, California 94720	1	Dr. Keith H. Johnson Massachusetts Institute of Technology Department of Metallurgy and Materials Science Cambridge, Massachusetts 02139	1
	Dr. L. N. Jarvis Surface Chemistry Division 4555 Overlook Avenue, S.W. Washington, D.C. 20375	1	Dr. M. S. Wrighton Massachusetts Institute of Technology Department of Chemistry Cambridge, Massachusetts 02139	1
	Dr. W. M. Risen, Jr. Brown University Department of Chemistry Providence, Rhode Island 02912	1	Dr. J. E. Demuth IBM Corp. Thomas J. Watson Research Center P.O. Box 218 Yorktown Heights, New York 10598	1
	Dr. M. H. Chisholm Princeton University Chemistry Department Princeton, New Jersey 08540	1	Dr. C. P. Flynn University of Illinois Department of Physics Urbana, Illinois 61801	1
	Dr. J. B. Hudson Rensselaer Polytechnic Institute Materials Division Troy, New York 12181	1	Dr. W. Kohn University of California (San Diego) Department of Physics La Jolla, California 92037	1
	Dr. John T. Yates National Bureau of Standards Department of Commerce Surface Chemistry Section Washington, D.C. 20234	1	Dr. R. L. Park Director, Center of Materials Research University of Maryland College Park, Maryland 20742	1
	Dr. Theodore E. Madey Department of Commerce National Bureau of Standards Surface Chemistry Section Washington, D.C. 20234	1		
	Dr. J. M. White University of Texas Department of Chemistry Austin, Texas 78712	1		

TECHNICAL REPORT DISTRIBUTION LIST

<u>No. Copies</u>		<u>No. Cop</u>
	Dr. W. T. Peria Electrical Engineering Department University of Minnesota Minneapolis, Minnesota 55455	1
	Dr. Leonard Wharton James Franck Institute Department of Chemistry 5640 Ellis Avenue Chicago, Illinois 60637	1
	Dr. Markis Tzoar City University of New York Convent Avenue at 138th Street New York, New York 10031	1
	Dr. M. G. Lagally Department of Metallurgical and Mining Engineering University of Wisconsin Madison, Wisconsin 53706	1
	Dr. Chia-wei Woo Northwestern University Department of Physics Evanston, Illinois 60201	1
	Dr. Robert Gomer James Franck Institute Department of Chemistry 5640 Ellis Avenue Chicago, Illinois 60637	1
	Dr. D. C. Mattis Yeshiva University Physics Department Amsterdam Avenue & 185th Street New York, New York 10033	1
	Dr. R. F. Wallis University of California (Irvine) Department of Physics Irvine, California 92664	1
	Dr. Robert M. Hexter University of Minnesota Department of Chemistry Minneapolis, Minnesota 55455	1

TECHNICAL REPORT DISTRIBUTION LIST

	<u>No. Copies</u>		<u>No. Copies</u>
Dr. Stephen H. Carr Department of Materials Science Northwestern University Evanston, Illinois 60201	1	Dr. G. Goodman Globe Union Inc. 5757 North Green Bay Avenue Milwaukee, Wisconsin 53201	1
Dr. M. Broadhurst Bulk Properties Section National Bureau of Standards U.S. Department of Commerce Washington, D.C. 20234	2	Picatinny Arsenal SMUPA-FR-M-D Dover, New Jersey 07801 Attn: A. M. Anzalone Bldg. 3401	1
Dr. C. H. Wang Department of Chemistry University of Utah Salt Lake City, Utah 84112	1	Dr. J. K. Gillham Princeton University Department of Chemistry Princeton, New Jersey 08540	1
Dr. T. A. Litovitz Department of Physics Catholic University of America Washington, D.C. 20017	1	Douglas Aircraft Co. 3855 Lakewood Boulevard Long Beach, California 90846 Attn: Technical Library C1 290/36-84 AUTO-Sutton	1
Dr. R. V. Subramanian Washington State University Department of Materials Science Pullman, Washington 99163	1	Dr. E. Baer Department of Macromolecular Science Case Western Reserve University Cleveland, Ohio 44106	1
Dr. M. Shen Department of Chemical Engineering University of California Berkeley, California 94720	1	Dr. K. D. Pae Department of Mechanics and Materials Science Rutgers University New Brunswick, New Jersey 08903	1
Dr. V. Stannett Department of Chemical Engineering North Carolina State University Raleigh, North Carolina 27607	1	NASA-Lewis Research Center 21000 Brookpark Road Cleveland, Ohio 44135 Attn: Dr. T. T. Serofini, MS-49-1	1
Dr. D. R. Uhlmann Department of Metallurgy and Material Science Center for Materials Science and Engineering Massachusetts Institute of Technology Cambridge, Massachusetts 02139		Dr. Charles H. Sherman, Code TD 121 Naval Underwater Systems Center New London, Connecticut	1
Naval Surface Weapons Center White Oak Silver Spring, Maryland 20910 Attn: Dr. J. M. Augl Dr. B. Hartman	1	Dr. William Risen Department of Chemistry Brown University Providence, Rhode Island 02912	1

	<u>No. Copies</u>		<u>No. Copies</u>
Dr. Alan Gent Department of Physics University of Akron Akron, Ohio 44304	1	Dr. W. A. Spitzig United States Steel Corporation Research Laboratory Monroeville, Pennsylvania 15146	1
Mr. Robert W. Jones Advanced Projects Manager Hughes Aircraft Company Mail Station D 132 Culver City, California 90230	1	Dr. T. P. Conlon, Jr., Code 3622 Sandia Laboratories Sandia Corporation Albuquerque, New Mexico 87115	1
Dr. C. Giori IIT Research Institute 10 West 35 Street Chicago, Illinois 60616	1	Dr. Martin Kaufmann, Head Materials Research Branch, Code 4542 Naval Weapons Center China Lake, California 93555	1
Dr. M. Litt Department of Macromolecular Science Case Western Reserve University Cleveland, Ohio 44106	1	Dr. T. J. Reinhart, Jr., Chief Composite and Fibrous Materials Branch Nonmetallic Materials Division Department of the Air Force Air Force Materials Laboratory (AFSC) Wright-Patterson Air Force Base, Ohio 45433	1
Dr. R. S. Roe Department of Materials Science and Metallurgical Engineering University of Cincinnati Cincinnati, Ohio 45221	1	Dr. J. Lando Department of Macromolecular Science Case Western Reserve University Cleveland, Ohio 44106	
Dr. L. E. Smith U.S. Department of Commerce National Bureau of Standards Stability and Standards Washington, D.C. 20234	1	Dr. J. White Chemical and Metallurgical Engineering University of Tennessee Knoxville, Tennessee 37916	1
Dr. Robert E. Cohen Chemical Engineering Department Massachusetts Institute of Technology Cambridge, Massachusetts 02139	1	Dr. J. A. Manson Materials Research Center Lehigh University Bethlehem, Pennsylvania 18015	1
Dr. David Roylance Department of Materials Science and Engineering Massachusetts Institute of Technology Cambridge, Massachusetts 02039	1	Dr. R. F. Helmreich Contract RD&E Dow Chemical Co. Midland, Michigan 48640	1

